

2013

Cannabinoid receptor 1 (CB1) agonist  
arachidonyl-2'-chloroethylamide (ACEA)  
induces Egr1 in murine 3T3-L1 and  
human adipocytes

---

<https://hdl.handle.net/2144/12255>

*Downloaded from DSpace Repository, DSpace Institution's institutional repository*

BOSTON UNIVERSITY

SCHOOL OF MEDICINE

Thesis

**CANNABINOID RECEPTOR 1 (CB1) AGONIST ARACHIDONYL-2'-  
CHLOROETHYLAMIDE (ACEA) INDUCES EGR1 IN MURINE 3T3-L1 AND  
HUMAN ADIPOCYTES**

by

**BRADLEY PRESTON ZEHR**

B.A., Indiana University, 2011

Submitted in partial fulfillment of the

requirements for the degree of

Master of Arts

2013

Approved by

First Reader \_\_\_\_\_

Konstantin V. Kandror, Ph.D.  
Professor of Biochemistry

Second Reader \_\_\_\_\_

Michael Y. Sherman, Ph.D.  
Professor of Biochemistry

## **ACKNOWLEDGEMENTS**

I thank Dr. Konstantin Kandror for graciously accepting me into his laboratory for the short duration of this master's thesis work. His expertise, guidance, patience, and kindness were profoundly helpful to me as I undertook my first laboratory research effort as a graduate student. I also want to thank Dr. Michael Sherman, my second reader, for donating his time to improving and approving this thesis work.

Thank you to the Kandror Lab members: Dr. Xiaoqing Yang for training me during the first month and always stopping her work when I needed assistance; Dr. Maneet Singh for providing incredible support and kindness on a daily basis; Dr. Yu-Kyong Shin for answering my frequent questions throughout the project; Dana Pena for her advice and critique on lab techniques; Jessica Kim for guidance through the MAMS program and thesis-writing; and Agnes Asmar for her friendship and support.

I thank the Graduate Medical Sciences Faculty and Staff for their assistance in navigating the MAMS program. In particular, I thank MAMS director Dr. Gwynneth Offner for giving me the opportunity to be Teaching Assistant for Biochemistry and Cell Biology; Dr. Vickery Trinkaus-Randall for serving as my academic adviser and inviting me to be a student mentor; Dr. Theresa Davies for communicating important information to the MAMS students; and Mildred Agosto for completing a format review of this thesis.

**CANNABINOID RECEPTOR 1 (CB1) AGONIST ARACHIDONYL-2'-  
CHLOROETHYLAMIDE (ACEA) INDUCES EGR1 IN MURINE 3T3-L1 AND  
HUMAN ADIPOCYTES**

**BRADLEY PRESTON ZEHR**

Boston University School of Medicine, 2013

Major Professor: Konstantin V. Kandror, Ph.D., Professor of Biochemistry

**ABSTRACT**

Obesity and type 2 diabetes mellitus are parallel global pandemics fueled by worldwide trends toward longer lifespan, Western high-fat diet, and sedentary lifestyle. Lipotoxicity – lipid overflow from adipose tissue to liver, muscle, and pancreas resulting from chronically elevated plasma free fatty acid levels – is now known to be the underlying cause of insulin resistance and T2DM. Control of lipolysis in adipose tissue is central to the regulation of plasma free fatty acid. Adipose triglyceride lipase (ATGL), the rate-limiting lipolytic enzyme in adipose tissue, is downregulated in the insulin-stimulated state, and this antilipolytic signal is defective in obesity and T2DM and may contribute to lipotoxicity. The antilipolytic insulin signal is mediated by mammalian target of rapamycin complex 1 (mTORC1), but how activated mTORC1 decreased ATGL expression remained elusive. The Kandror Lab recently identified transcription factor early growth responsive gene 1 (Egr1) as the missing link between insulin-activated mTORC1

and decreased ATGL expression. mTORC1 induces Egr1, which directly binds the ATGL promoter and decreases its expression.

Intriguingly, Egr1 has also been implicated in a new model of the pathogenesis of insulin resistance in the pre-diabetic hyperinsulinemic state. Several groups have demonstrated that chronic hyperinsulinism causes an imbalance between PI3K/Akt signaling and MAPK signaling, and this defect is mediated by high levels of Egr1 in obesity. Additionally, the endocannabinoid system (ECS) is known to be hyperactive in obesity and diabetes, and antagonism of cannabinoid receptor 1 (CB1) by pharmaceutical rimonabant was effective at decreasing weight and improving insulin resistance in overweight and obese patients. Previous research demonstrated induction of Egr1 by CB1 stimulation in neurons, however the same effect has not been demonstrated in adipocytes.

We stimulated murine 3T3-L1 and human adipocytes with 2  $\mu$ M arachidonyl-2'-chloroethylamide (ACEA), a synthetic analogue of major endocannabinoid anandamide and a specific CB1 agonist. Egr1 mRNA was significantly increased in ACEA-stimulated murine and human adipocytes relative to controls after 4 hours, as analyzed by quantitative polymerase chain reaction. This finding potentially implicates hyperactive ECS during obesity in the pathogenesis of insulin resistance, and it further validates CB1 as a rich diabetes drug target.

## TABLE OF CONTENTS

	Page
Title	i
Reader's Approval Page	ii
Acknowledgements	iii
Abstract	iv
Table of Contents	vi
List of Figures	viii
List of Abbreviations	ix
Introduction	1
1. Obesity, Diabetes, and Public Health	1
2. Pathogenesis of Insulin Resistance and T2DM	3
3. Lipolysis in Adipose Tissue	5
3.1 Adipose Triglyceride Lipase	6
3.2 Lipolysis Stimulation and Suppression	7
3.3 Insulin-PI3K-Akt-TSC2-mTOR Axis	10
3.4 Post-Translational Regulation of ATGL	14
3.5 Transcriptional Regulation of ATGL	15
a. Egr1	15
b. IRF4, FoxO1, PPAR $\gamma$	17
4. PI3K/Akt and MAPK Signaling Imbalance in Insulin Resistance	18
5. Endocannabinoid System	21

5.1 Cannabinoid Receptors	21
5.2 Agonists and Antagonists	21
5.3 Rimonabant	25
5.4 Egr1	25
6. Thesis Objective	26
Materials and Methods	28
Murine 3T3-L1 Adipocyte Differentiation	28
Human Adipocyte Differentiation	28
Arachidonyl-2'-chloroethylamide (ACEA) Stimulation	29
Insulin Stimulation	29
Humulin Stimulation	30
Western Blot Analysis of ATGL and Egr1 in Murine 3T3-L1 Adipocytes and Human Adipocytes	30
RNA Extraction After Stimulation of Adipocytes	32
Reverse Transcription of RNA to cDNA	33
Analysis of mRNA Expression Using Quantitative Polymerase Chain Reaction	33
qPCR Data Analysis and Statistics	34
Results	35
Discussion	40
References	45
Vita	52



## LIST OF FIGURES

Figure	Title	Page
1	Diabetes prevalence in United States	2
2	Phosphorylation targets of Akt	10
3	Insulin activates mTORC1 via PI3K/Akt	12
4	ATGL and Egr1 expression during insulin time course	17
5	PI3K/Akt – MAPK imbalance in hyperinsulinemia	20
6	Structures of endocannabinoids	23
7	Structures of exogenous cannabinoids	24
8	ACEA induces Egr1 in murine 3T3-L1 adipocytes	37
9	ACEA does not affect Egr1 or ATGL protein	38
10	Insulin and ACEA induce Egr1 in human adipocytes	39
11	ACEA increases ATGL protein in human adipocytes	40

## ABBREVIATIONS

$\Delta$ 9-THC	$\Delta$ 9-tetrahydrocannabinol
2-AG	2-arachidonyl glycerol
4EBP1	eukaryotic initiation factor (eIF) 4E binding protein 1
ACEA	arachidonyl-2'-chloroethylamide
AEA	N-arachidonyl ethanolamine, also called anandamide
AMP	adenosine monophosphate
AMPK	AMP-activated protein kinase
Akt/PKB	protein kinase B
AT	adipose tissue
ATGL	adipose triglyceride lipase
BAT	brown adipose tissue
$\beta$ AR	beta adrenergic receptor
cAMP	cyclic adenosine monophosphate
CB1	cannabinoid receptor 1
CGI-58	comparative gene identification-58
DAG	diacylglyceride
DMEM	Dulbecco's modified Eagle's medium
ECS	endocannabinoid system
Egr1	early growth responsive gene 1
eIF4F	eukaryotic translation initiation factor 4F

ERK	extracellular signal-regulated kinase, also called MAPK
FBS	fetal bovine serum
FFA	free fatty acid
FoxO1	forkhead box O1
GAPDH	glyceraldehyde 3-phosphate dehydrogenase
GLUT4	glucose transporter type 4
G0S2	G0/G1 switch gene 2
GAP	GTPase-activating protein
GGPP	geranyl geranyl pyrophosphate
GGPPS	geranyl geranyl pyrophosphate synthase
GPCR	G protein-coupled receptor
HFD	high fat diet
hGP	hepatic glucose production
HSL	hormone sensitive lipase
IL-6	interleukin-6
IR	insulin receptor
IRF4	interferon regulatory factor 4
IRS1	insulin receptor substrate-1
LPL	lipoprotein lipase
MAG	monoacylglyceride
MAPK	mitogen-activated protein kinase, also called ERK
MEF	mouse embryonic fibroblast

MGL	monoacylglycerol lipase
mTORC1/2	mammalian target of rapamycin complex 1/2
NEFA	non-esterified fatty acid
PCR	polymerase chain reaction
PDK1	phosphoinositide-dependent kinase 1
PH	pleckstrin homology domain
PI3K	phosphatidylinositol 3-kinase
PIP3	phosphatidylinositol (3,4,5)-triphosphate
PKA	protein kinase A
PPAR $\gamma$	peroxisome proliferator-activated receptor $\gamma$
PTEN	phosphatase and tensin homolog
qPCR	quantitative polymerase chain reaction
Rheb	ras homologue enriched in brain
RPS18	40S ribosomal protein S18
S6K1	ribosomal protein S6 kinase 1
SH2	Src homology 2 domain
siRNA	small interfering RNA
SIRT1	sirtuin-1
T1DM	type 1 diabetes mellitus
T2DM	type 2 diabetes mellitus
TAG	triacylglyceride
TNF- $\alpha$	tumor necrosis factor-alpha

TSC1/2	tuberous sclerosis complex 1/2
TZD	thiazolidinedione
UCP1	uncoupling protein 1
VLDL	very low density lipoprotein
WAT	white adipose tissue
WT	wild-type

## **INTRODUCTION**

### **1. Obesity, Diabetes, and Public Health**

Obesity and Type 2 Diabetes Mellitus (T2DM) are twin global health pandemics [1]. The two diseases are intricately and definitively linked, to the extent that the term “diabesity” has entered the popular media lexicon [2]. In the United States, 18.8 million people were living with diagnosed diabetes and 7 million with undiagnosed diabetes in 2010, for a national diabetes prevalence of 8.3 percent. An additional 79 million Americans in 2010 exhibited pre-diabetic signs such as elevated fasting glucose and hemoglobin A1c levels [3]. Figure 1 demonstrates the dramatic increase in diabetes prevalence in the United States, especially since 1990 [4]. Globally, the number of people living with diabetes doubled between 1980 and 2008, from 153 million to 347 million [1]. Although approximately 70 percent of the increase is attributed to population growth and longer lifespan, a fundamental driver of the diabetes pandemic is increased prevalence of obesity secondary to Western diet, overeating, and sedentary lifestyle [1].

Complications of diabetes are numerous. Diabetes deteriorates the vasculature and increases risk of heart disease, heart attack, stroke, blindness, nephropathy, and neuropathy; poor perfusion of the lower extremities increases risk of ulcer, gangrene, and amputation of the foot [3]. Diabetes is currently the seventh leading cause of death in the United States, and of the 15 leading

causes of U.S. deaths, diabetes had the second-largest increase in death rate between 2010 and 2011 (3.4 percent) [5].

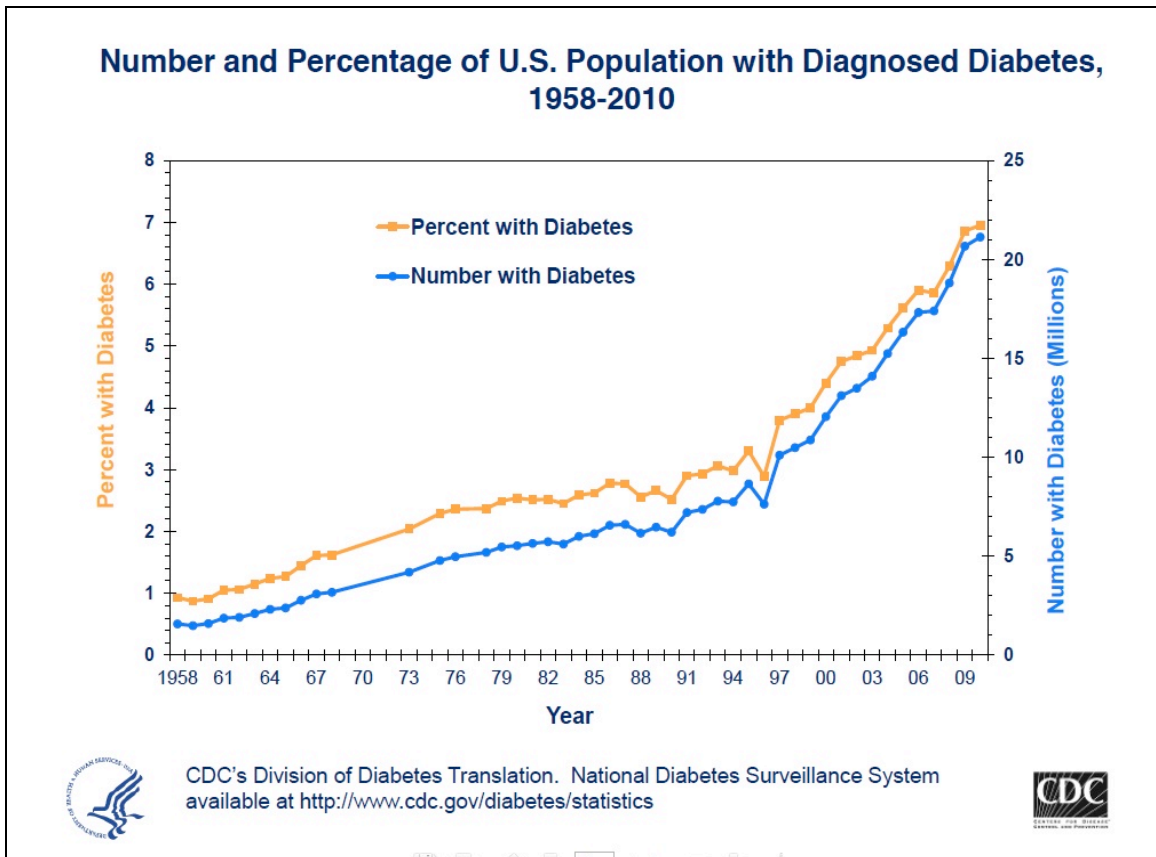


**Figure 1. Diabetes prevalence in United States.** Number and percentage of Americans living with diabetes has increased drastically in the past two decades. Figure taken from “Long-Term Trends in Diagnosed Diabetes”, Centers for Disease Control and Prevention, 2011 [4].

## **2. Pathogenesis of Insulin Resistance and T2DM**

Both Type 1 and Type 2 Diabetes Mellitus manifest as impaired glucose tolerance and fasting hyperglycemia. T1DM is caused by insulin deficiency due to autoimmune destruction of the pancreatic  $\beta$ -cells, and T2DM is caused by insulin insensitivity and resistance in muscle, liver, and fat tissue. T1DM, formerly labeled “juvenile onset” and “insulin-dependent”, presents in early life, most commonly during adolescence, and patients are dependent on lifelong subcutaneous injection of insulin. T2DM, formerly labeled “adult onset” and “non-insulin-dependent”, classically presents in older adults and geriatric patients and is strongly associated with overweight and obesity. However, the diabetes and obesity epidemic has lowered the average age of T2DM onset to middle adulthood and has recently expanded to the young adult and pediatric populations. T2DM accounts for approximately 95 percent of all adult diabetes cases [3]. The remainder of this paper specifically addresses T2DM.

The term “diabetes mellitus” derives from Latin and Greek and means excessive urine with a honey-sweet taste, and the condition has been known since antiquity. In the 1880s, Oskar Minkowski documented sweetness in the urine of pancreatectomized dogs, concluding that the pancreas secretes a substance critical for the regulation of blood glucose [6]. After Dr. Frederick Banting isolated insulin from pancreatic  $\beta$ -cells in 1921, the concept of regulation of blood glucose by insulin was firmly established in medicine, and thereafter diabetes was viewed primarily as a disorder of carbohydrate metabolism [6]. In



his paradigm-shifting 1992 *Science* paper, Dr. John McGarry asked how diabetes research might be different if Minkowski had smelled acetone (a byproduct of ketoacids) in the urine rather than tasted sugar, and McGarry argued that the role of lipid metabolism dysregulation had been underappreciated in the pathogenesis of insulin resistance and diabetes [6].

Insulin resistance is now understood to arise primarily from defects in lipid metabolism [7]. Lipotoxicity, a term introduced by Unger and McGarry in 1994, is the aberrant accumulation of lipids in non-adipose tissue, particularly in liver, muscle, and pancreatic  $\beta$ -cell, following increased plasma free fatty acid (FFA) levels [8]. Unger proposed that increased plasma FFA had parallel effects of increasing insulin secretion (hyperinsulinemia) and increasing peripheral insulin resistance long before diagnosis of overt diabetes [9]. Dresner et al. demonstrated that elevated plasma FFA induced insulin resistance in humans by diminishing insulin signal transduction through the phosphatidylinositol 3-kinase (PI3K) pathway [10]. Elevated plasma FFA may represent caloric intake in excess of the triacylglycerol (TAG) storage capacity of adipose tissue; high FFA increases ectopic TAG accumulation and causes subsequent metabolic dysfunction of tissues such as muscle, liver, and pancreatic  $\beta$ -cell [11].

Chronically elevated plasma FFA decreases insulin secretion by pancreatic  $\beta$ -cells [12], decreases insulin-stimulated glucose uptake by skeletal muscle [13], decreases insulin-stimulated suppression of hepatic glucose production (hGP) by gluconeogenesis [13], and decreases insulin-stimulated

suppression of lipolysis in adipose tissue [14]. All of these effects contribute to the “metabolic syndrome”, a state of hyperlipidemia, hypercholesterolemia, ectopic adiposity, insulin resistance, and hyperglycemia [15]. Therefore, precise regulation of plasma FFA concentration is vitally important to maintain normal metabolic function and prevent the pathogenesis of insulin resistance and diabetes mellitus.

### **3. Lipolysis in Adipose Tissue**

Among the several contributors to increased plasma FFA levels in obesity and diabetes, dysregulated lipolysis in adipose tissue (AT) is central [16]. In normal physiology, the fasted state induces lipolysis in the adipocyte lipid droplet (LD) and release of FFA into circulation. FFA is then used by the liver and muscle for mitochondrial  $\beta$ -oxidation and by the liver for ketogenesis. The fed state suppresses lipolysis in AT and stimulates uptake of plasma glucose by muscle, liver, and AT. LDs are present in all cell types and occupy minor volume, approximately 1 micron, providing a small TAG and cholesteryl ester depot for use by individual cells. In white adipose tissue (WAT), LDs are approximately 50 microns and occupy nearly the entire cell, providing TAG energy storage for the whole organism [17].

### **3.1 Adipose Triglyceride Lipase**

Until 2004, the two major lipases characterized in AT were monoglyceride lipase (MGL) and hormone-sensitive lipase (HSL). HSL is selective for diacylglycerides (DAG) and catalyzes the hydrolysis of one of the two acyl groups on DAG, resulting in one FFA and one monoacylglyceride (MAG). HSL also has some TAG hydrolysis activity but has much higher affinity for DAG substrates. MGL is selective for MAG and catalyzes the hydrolysis of the final acyl group from glycerol, releasing one FFA and glycerol. Of these two lipases, HSL was viewed as the rate-limiting lipolytic enzyme in AT. Vaughan et al. wrote in 1964, "It seems reasonable to conclude that activation of the hormone-sensitive lipase system accounts for wholly or in large part for the fat-mobilizing action of epinephrine, norepinephrine, ACTH, glucagon, and TSH [18]." In 2001, Haemmerle et al. showed HSL-null mice exhibited decreased lipolysis but accumulation of DAG and not TAG in AT, indicating the existence of a third lipase in AT specific for TAG conversion to DAG [19].

Three groups reported the identification of adipose triglyceride lipase (ATGL) in 2004, an AT lipase selective for TAG hydrolysis to DAG [20] [21] [22]. Together, ATGL and HSL account for 95 percent of lipolysis in WAT [23]. ATGL is now known to be the rate-limiting enzyme in AT lipolysis [24]. Inactivation of ATGL in mice leads to dramatically increased adiposity throughout the body and causes premature death because of cardiac dysfunction [25]. These mice are also impaired in maintaining body temperature during cold as the availability of

plasma FFA for use in brown adipose tissue (BAT) thermogenesis is decreased [25]. As predicted by the lipotoxicity model, decreased plasma FFA in these mice increases insulin sensitivity and glucose tolerance [25]. In fact, ATGL-null mice are protected against high-fat diet (HFD) induced insulin resistance and glucose intolerance despite weight gain [26].

Conversely, transgenic mice overexpressing ATGL are leaner with decreased TAG accumulation and smaller adipocytes secondary to increased lipolysis [27]. Intriguingly, these mice do not exhibit increased plasma FFA. Rather, genes for mitochondrial  $\beta$ -oxidation, peroxisomal  $\alpha$ -oxidation, and thermogenesis are up-regulated in their adipocytes, including a 7-fold increase of uncoupling protein 1 (UCP1) and consequent higher body temperature [27]. These mice also show increased insulin sensitivity despite unchanged plasma FFA levels relative to control wild-type (WT) mice, indicating plasma FFA concentration is not the sole determinant of insulin sensitivity.

### **3.2 Lipolysis Stimulation and Suppression**

The major stimulus for lipolysis in AT is activation of the  $\beta$ -adrenergic receptor ( $\beta$ AR) by catecholamines epinephrine and norepinephrine [28]. Stimulation of  $\beta$ AR, a G protein-coupled receptor (GPCR), activates adenylate cyclase, which catalyzes the conversion of adenosine monophosphate (AMP) to cyclic AMP (cAMP). Increased intracellular concentration of cAMP activates protein kinase A (PKA). Activated PKA induces lipolysis through several

effectors. PKA phosphorylates HSL, which activates the translocation of HSL to the LD where it can participate in lipolysis. PKA phosphorylates perilipin, a constituent “guardian protein” located at the LD-cytosol interface, leading to the release of CGI-58 from perilipin. CGI-58 is a co-activator of ATGL, and its release from phosphorylated perilipin increases ATGL activity 20-fold [29].

Tumor necrosis factor- $\alpha$  (TNF- $\alpha$ ) also stimulates lipolysis, and the effect is mediated by G0S2 (G0/G1 switch gene 2), a selective inhibitor of ATGL [30]. TNF- $\alpha$  decreases transcription of G0S2, thus relieving ATGL of G0S2 inhibition and stimulating lipolysis. Glucocorticoids are also thought to stimulate lipolysis in AT, although this effect is somewhat ambiguous and its mechanism not definitively elucidated [31].

Recently, Sirtuin-1 (SIRT1), a protein deacetylase, was found to stimulate AT lipolysis [32]. SIRT1 is activated during fasting and deacetylates transcription factor forkhead box O1 (FoxO1), which can then directly bind the ATGL promoter and transactivate ATGL gene transcription. This effectively increases AT lipolysis. AMP-activated protein kinase (AMPK) has been implicated in stimulation of lipolysis, but Kandror et al. found no effect on lipolysis in a cell line with dominant-negative catalytic subunits of AMPK [32].

The major suppressor of lipolysis in AT is insulin [24]. The major mediator of insulin signal transduction is Akt, also called protein kinase B (PKB). Akt has myriad cellular targets, as shown in Figure 2 [33]. The three targets most relevant to insulin-stimulated suppression of AT lipolysis are tuberous sclerosis complex 2

(TSC2), FoxO1, and cyclic nucleotide phosphodiesterase-3b (PDE-3b) (not shown in Figure 2). Akt phosphorylates and activates PDE-3b, which catalyzes the conversion of cAMP to AMP, reversing the effect of catecholamine stimulation of  $\beta$ AR and suppressing lipolysis [34]. Akt phosphorylates the transcription factor FoxO1, which sequesters FoxO1 outside the nucleus, thus rendering it incapable of binding and activating the ATGL promoter [35]. Akt phosphorylates and inhibits TSC2, leading to the activation of mammalian target of rapamycin complex 1 (mTORC1) [36], a canonical signaling pathway discussed in the next section. Insulin also activates the canonical mitogen-activated protein kinase (MAPK) pathway [37], the effects of which are discussed in later sections.

A second suppressor of lipolysis in AT is adiponectin, an autocrine hormone secreted by AT. Adiponectin is viewed a “sensitizer” of insulin antilipolytic activity, but recent reports show adiponectin also inhibits lipolysis independent of insulin signaling [38]. High levels of the FFA palmitate decrease adiponectin expression and secretion and also induce lysosomal degradation of adiponectin [39].

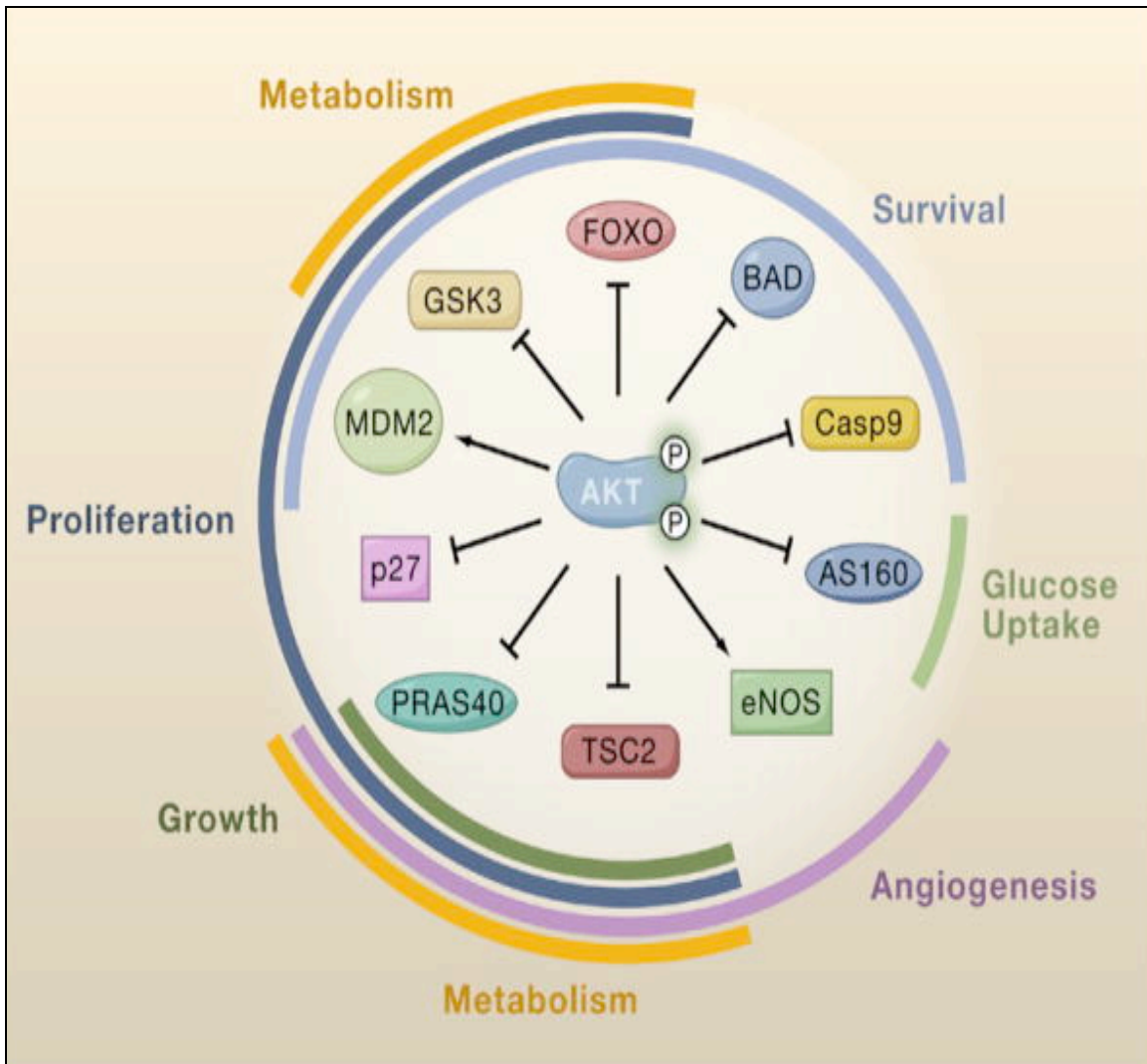


**Figure 2. Phosphorylation targets of Akt.** Akt/PKB, the major effector of insulin signal transduction in AT, is a central mediator of myriad cellular processes. FoxO and TSC2 are especially relevant to insulin-stimulated suppression of lipolysis. FoxO – forkhead box O; TSC2 – tuberous sclerosis complex 2. Figure taken from Manning and Cantley, 2007.

### 3.3 Insulin-PI3K-Akt-TSC2-mTOR Axis

The activation of mTORC1 by insulin is a highly investigated insulin signaling pathway and is illustrated in Figure 3 [33]. Briefly, insulin binds insulin receptor (IR), a receptor tyrosine kinase (RTK), causing dimerization and

autophosphorylation of IR on tyrosine residues. IR recruits and phosphorylates insulin receptor substrate 1 (IRS1) on specific tyrosine residues. Phosphorylated IR and IRS1 recruit PI3K and Grb2 to the cell membrane and both IR and IRS1 phosphorylate and activate PI3K and Grb2. Activated Grb2 (not shown in Figure 3) activates the MAPK pathway [40]. Activated PI3K phosphorylates the membrane phospholipid PIP2, producing PIP3. Both Akt and phosphoinositide-dependent kinase 1 (PDK1) are able to bind PIP3 via their pleckstrin homology (PH) domains. Akt is phosphorylated at Thr-308 by PDK1 and at Ser-473 by mTORC2. Both phosphorylation modifications are required for the full effector capabilities of Akt [41].

Akt phosphorylates TSC2 at multiple residues suppressing its biological activity. TSC2 is a GTPase-activating protein (GAP) for the small GTP-bound protein Rheb (Ras homolog enriched in brain, a misnomer as Rheb is found in non-brain tissue such as AT). Rheb directly stimulates mTORC1. Therefore, activated Akt stimulates mTORC1 by inhibiting an inhibitor (TSC2) of Rheb.



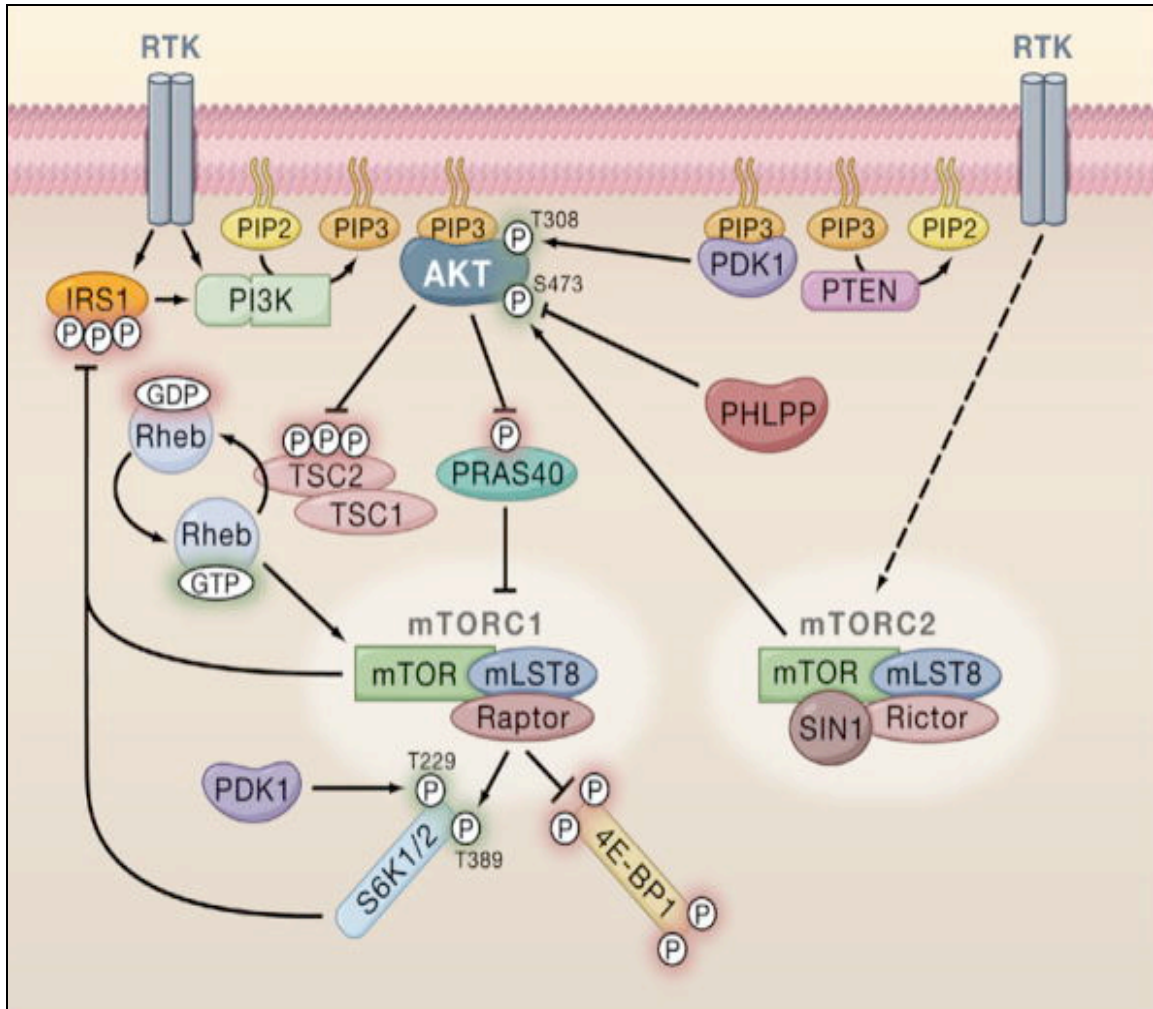


**Figure 3. Insulin activates mTORC1 via PI3K/Akt.** Solid lines represent direct interaction and dotted lines represent indirect effects with unillustrated mediators. RTK – receptor tyrosine kinase; PI3K – phosphatidylinositol 3-kinase; PIP3 – phosphatidylinositol (3,4,5)-triphosphate; TSC2 – tuberous sclerosis complex 2; Rheb – ras homolog enriched in brain; mTOR – mammalian target of rapamycin; PDK1 – phosphoinositide-dependent kinase 1; PTEN – phosphatase and tensin homolog; IRS1 – insulin receptor substrate 1; S6K1 – ribosomal S6 protein kinase 1; 4EBP1 – eukaryotic initiation factor (eIF) 4E binding protein. Figure taken from Manning and Cantley, 2007.

Although many interesting details about the PI3K-Akt-TSC2-mTOR pathway are beyond the scope of this paper, several aspects require emphasis. Firstly, embedded in the pathway is a negative feedback signal. mTORC1 phosphorylates and activates ribosomal protein S6 kinase 1 (S6K1), which in turn phosphorylates several substrates, including IRS1 [42]. This modification of IRS1 at multiple serine residues decreases IRS1 binding to IR, decreases PI3K activation, and decreases the overall PI3K-Akt signal. Foster et al. hypothesized that overactive mTORC1 secondary to hyperinsulinemia in obesity decreases PI3K-Akt signaling through the S6K1-IRS1 mechanism and contributes to insulin resistance [41].

Secondly, insulin also activates the MAPK signal cascade (not shown in Figure 3), and the MAPK pathway also activates mTORC1 [37], which will be important for the later discussion about transcription factor early growth responsive gene 1 (Egr1).

Thirdly, and to the earlier point about insulin-stimulated suppression of lipolysis in AT, insulin decreases transcription of ATGL in an mTORC1-dependent manner [36]. Constitutive activation of mTORC1 via insertion of a Rheb transgene decreases transcription of ATGL, suppresses lipolysis, and increases intracellular TAG. Similarly, TSC2-null mouse embryonic fibroblasts (MEFs), which exhibit overactive mTORC1, also show decreased transcription of ATGL and suppression of lipolysis. Conversely, inhibition of mTORC1 by rapamycin induces ATGL transcription and increases lipolysis [36]. The

transcription factor through which mTORC1 down regulates ATGL expression has been identified as Egr1 by the Kandror Lab, although the paper has yet to be published.

### **3.4 Post-Translational Regulation of ATGL**

Because ATGL is the rate-limiting lipolytic enzyme in AT, and because AT lipolysis is a central contributor to plasma FFA levels, ATGL regulation is of keen importance in diabetes research. As discussed earlier, ATGL activity is inhibited by direct interaction with G0S2, a protein most highly expressed in AT and liver [28]. Knockdown of G0S2 increases both basal and  $\beta$ AR-stimulated lipolysis, and overexpression of G0S2 decreases lipolysis [30]. Recently, Schweiger et al. confirmed G0S2 interaction with and inhibition of ATGL in human adipocytes [43]. Also discussed earlier was CGI-58, a protein activator of ATGL. CGI-58 directly interacts with ATGL and is required for the full activation of ATGL. Mutations in CGI-58 cause Chanarin-Dorfman Syndrome, which is characterized by excessive TAG accumulation in multiple tissues [29].

AMPK phosphorylates ATGL at Ser-406, which increases ATGL activity. However, different groups have shown AMPK activation to increase, decrease, or have no effect on lipolysis [32]. Unlike HSL, ATGL is not phosphorylated by PKA or MAPK [28].

Another possible regulator of ATGL at the protein level is the insulin-stimulated degradation of ATGL by ubiquitination and selective autophagy.

Activated IRS1 is known to bind the Src homology 2 (SH2) domain of p62, an adaptor protein involved in joining ubiquitinated proteins with autolysosomal proteins [40]. Furthermore, some preliminary data from the Kandror Lab suggests that ATGL interacts with parkin, an E3 ubiquitin ligase, upon insulin stimulation. However, the role of autophagy in ATGL regulation is not clear.

### **3.5 Transcriptional Regulation of ATGL**

Three transcription factors bind to and activate the ATGL gene promoter: IRF4, FoxO1, and PPAR $\gamma$ . Recently, Kandror et al. identified Egr1 as a fourth transcription factor that binds the ATGL promoter but has an inhibitory effect on ATGL expression. Data supporting this claim are under review for publication.

#### ***a. Egr1***

Egr1 binds the ATGL promoter and decreases ATGL expression. Kandror et al. found that Egr1 is the mediator of mTORC1 suppression of ATGL transcription in the insulin-stimulated state (unpublished data). WT MEFs and TSC2-null MEFs were transfected with luciferase cDNA linked to ATGL promoter. In TSC2-null MEFs, mTORC1 was hyperactivated, and luciferase expression was decreased significantly relative to WT MEFs, supporting the previous finding that insulin-activated mTORC1 decreases ATGL expression. Rapamycin treatment of yeast inhibited mTORC1 and increased ATGL mRNA. A yeast genetic screen identified Msn4 as a transcription factor that suppresses ATGL

gene transcription. The mammalian homologue for Msn4 is Egr1, also called Krox24. Co-transfection of ATGL promoter-linked luciferase cDNA and Egr1 cDNA in HEK-293T cells significantly decreased luciferase expression relative to empty vector.

During a time course study of mRNA and protein levels of ATGL and Egr1 in 3T3-L1 adipocytes, Kandror et al. found that Egr1 mRNA levels increased dramatically after 4 hours of insulin stimulation (Figure 4). After 8 hours of insulin, Egr1 mRNA was lower than at 4 hours but Egr1 protein levels were increased significantly. At 8 hours, there was no change in ATGL protein level but significantly decreased ATGL mRNA. By 16 hours of insulin stimulation, Egr1 mRNA and protein levels returned to baseline, ATGL mRNA levels similar were to the 8-hour time point, but ATGL protein was significantly decreased. This study demonstrates that suppression of ATGL protein is subsequent to induction of Egr1 in the insulin-stimulated state. Chromatin immunoprecipitation (ChIP) verified the direct binding of Egr1 protein to ATGL promoter. Rapamycin, the mTORC1 inhibitor, blocked insulin-induced Egr1 expression and rescued ATGL from insulin-stimulated down-regulation.

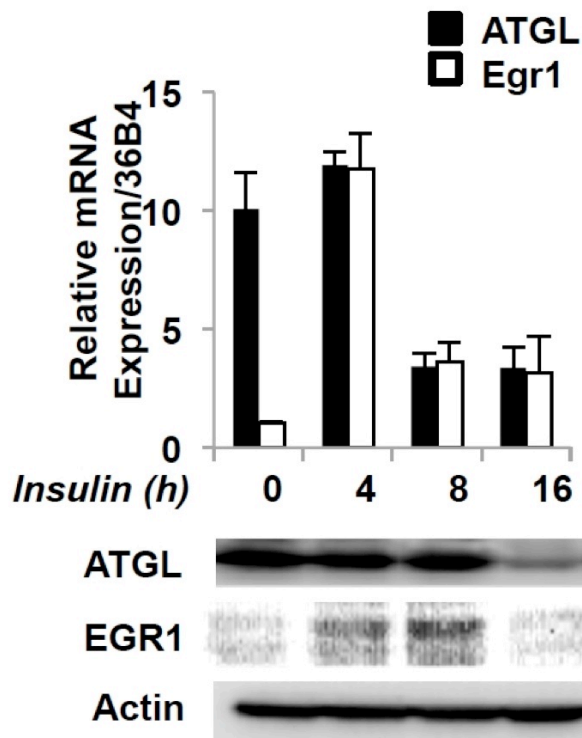


**Figure 4. ATGL and Egr1 expression during insulin time course.** 3T3-L1 adipocytes treated with 100 nM insulin for the time periods shown. Levels of ATGL and Egr1 mRNA measured in triplicate by quantitative PCR and normalized by 36B4 mRNA. Levels of ATGL and Egr1 protein measured by Western blot with actin as loading control. ATGL – adipose triglyceride lipase; Egr1 – early growth responsive gene 1. Figure taken from unpublished Kandror et al data.

***b. IRF4, FoxO1, PPAR $\gamma$***

Interferon regulatory factor 4 (IRF4) binds the ATGL promoter and transactivates the ATGL gene, and insulin signaling inhibits IRF4 transactivation of ATGL [44]. The ATGL promoter also contains two canonical FoxO1 binding sites, and Kandror et al. demonstrated that co-transfection of FoxO1 and

luciferase gene with ATGL promoter led to expression of luciferase [35].

Knockdown of FoxO1 in 3T3-L1 adipocytes decreased ATGL expression, basal lipolysis, and  $\beta$ AR-stimulated lipolysis. Conversely, transfection of MEFs with FoxO1-containing lentivirus increased ATGL expression. SIRT1, which is active during fasting, deacetylates and activates FoxO1, leading to increased ATGL expression and lipolysis [32]. Insulin-stimulated Akt phosphorylates FoxO1, thus excluding FoxO1 from the nucleus and inhibiting its ATGL promoting activity [35].

The peroxisome proliferator-activated receptor  $\gamma$  (PPAR $\gamma$ ) transactivates ATGL gene expression by binding the ATGL promoter [45]. The PPAR family contains 4 members that are nuclear receptor transcription factors whose ligands include fatty acids, acyl-CoAs, glycerol phospholipids, and eicosanoids [28]. PPAR $\gamma$  is expressed most highly in WAT. PPAR $\gamma$  agonists such as rosiglitazone and the thiazolidinedione (TZD) anti-diabetic drugs increase ATGL mRNA and protein, and this effect is demolished by antagonism or siRNA knockdown of PPAR $\gamma$  [46].

#### **4. PI3K/Akt and MAPK Signaling Imbalance in Insulin Resistance**

As discussed previously, insulin activates both the PI3K/Akt and MAPK signal cascades in AT. Both Akt and MAPK – also called extracellular signal-regulated kinase (ERK) – phosphorylate and inhibit TSC2, leading to the activation of mTORC1 [47] and increased expression of Egr1. Egr1 expression is increased in ob/ob mice and in the AT of diabetic patients [37]. Concordant with

this observation, obese patients and T2DM patients exhibit decreased expression of ATGL, as do the mouse models of obesity (ob/ob mice) and diabetes (db/db mice) [48].

Shen et al. present a model that depicts the role of elevated Egr1 in the development of imbalance between PI3K/Akt and MAPK signaling [37]. Chronic hyperinsulinemia, as experienced by pre-diabetic patients, leads to chronically elevated Egr1 levels in AT. Egr1 transactivates the gene for geranyl geranyl pyrophosphate synthase (GGPPS), which catalyzes the synthesis of 20-carbon quadruple isoprene molecule called geranyl geranyl pyrophosphate (GGPP). GG is a prenylation (anchoring) moiety added to Ras, the small GTPase, to increase cell membrane anchoring and thus enhance MAPK signaling as shown in Figure 5. Concurrently, activated ERK phosphorylates IRS1 at Ser-612, which diminishes insulin signal transduction through the PI3K/Akt pathway. Chronic hyperinsulinemia therefore increases MAPK signaling but decreases PI3K/Akt insulin signaling in an Egr1-dependent mechanism. Shen et al. demonstrated that insulin sensitivity could be restored in previously insulin-resistant adipocytes by any of the following: 1) Egr1 ablation; 2) GGPPS knockdown; 3) ERK inhibition [37].

In addition to the Egr1-GGPPS mechanism of PI3K/Akt – MAPK imbalance in pre-diabetic hyperinsulinemia, Xiao et al. introduced a second mechanism [49]. Egr1 also transactivates the phosphatase and tensin homologue (PTEN) gene, whose protein product dephosphorylates PIP3 and



inhibits PI3K/Akt signal transduction. As above, pre-diabetic hyperinsulinism increases Egr1 expression in AT, which increases MAPK signaling via the GGPPS-Ras mechanism and decrease PI3K/Akt signaling via IRS1 phosphorylation and PTEN induction. Furthermore, Sartipy et al. found that Egr1 is one of a few genes that remain insulin-sensitive during the development of adipocyte insulin resistance [50]. Thus, Egr1 is emerging as a critical mediator in the development of insulin resistance and T2DM.

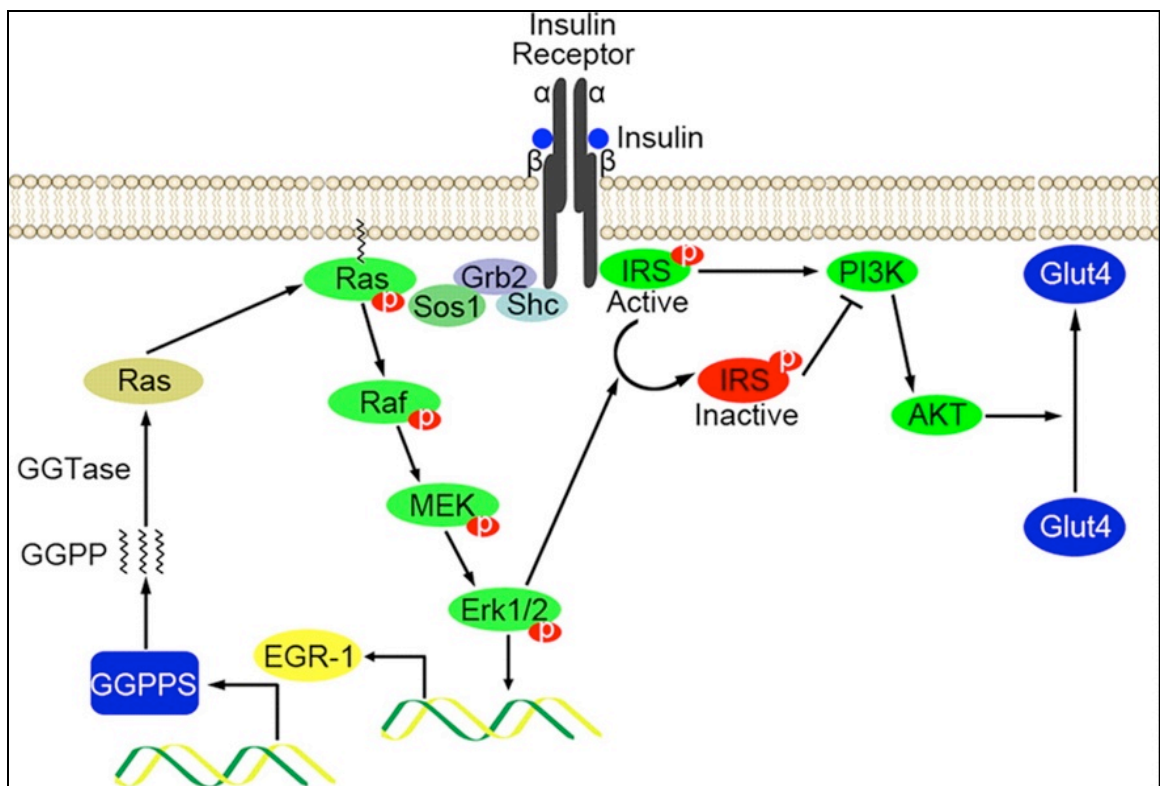


**Figure 5. PI3K/Akt – MAPK imbalance in hyperinsulinemia.** GGPPS – geranyl geranyl pyrophosphate synthase; PI3K – phosphatidylinositol 3-kinase; Egr1 – early growth response gene 1; Erk – extracellular signal-regulated kinase; IRS1 – insulin receptor substrate 1; GGTase – geranyl geranyl transferase. Figure taken from Shen, et al. 2011.

## **5. Endocannabinoid System**

The endocannabinoid system (ECS), as its name hints, was first investigated in relation to the psychotropic effects of the smoking plant *Cannabis sativa*, or marijuana. The psychoactive compound in marijuana,  $\Delta^9$ -tetrahydrocannabinol ( $\Delta^9$ -THC), binds cannabinoid receptors in the brain to produce euphoria and stimulate appetite, among other effects. The ECS has become a major diabetes research topic because ECS is hyperactive in obesity and T2DM, and pharmacologic blockade of the ECS has been shown to improve insulin resistance and overall lipid metabolism in mouse and human trials [51].

### **5.1 Cannabinoid Receptors**

Cannabinoid receptors are classical 7-transmembrane GPCRs, and there are two subtypes: CB1 and CB2. CB1 was traditionally labeled the “brain type”, but current research has found CB1 expression in a large variety of tissues including AT. CB2 is only expressed in immunity and inflammatory cells, with the exception of keratinocytes [52]. Among the multiple downstream effectors of CB1 activation, a major one is ERK [53].

### **5.2 Agonists and Antagonists**

Endocannabinoids are endogenous agonists of cannabinoid receptors. The first endocannabinoid to be identified was N-arachidonyl ethanolamine (AEA) in 1992 [52], followed later by identification of 2-arachidonyl glycerol (2-AG). AEA, also called anandamide from the *Sanskrit* meaning “bliss”, and 2-AG

are the two most important endocannabinoids, although others have been identified as shown in Figure 6. All of these molecules contain a 20-carbon arachidonyl moiety derived from arachidonic acid [54].

HU210 is a synthetic analogue to  $\Delta^9$ -THC and is the most potent CB1 agonist currently available [52]. CP-55940 is also a synthetic  $\Delta^9$ -THC mimetic and CB1 agonist. Arachidonyl-2'-chloroethylamide (ACEA) is a synthetic analogue to AEA and a selective CB1 agonist. SR141716A is a synthetic selective CB1 antagonist. The generic drug name for SR141716A is rimonabant. Natural  $\Delta^9$ -THC and the synthetic molecules are illustrated in Figure 7.

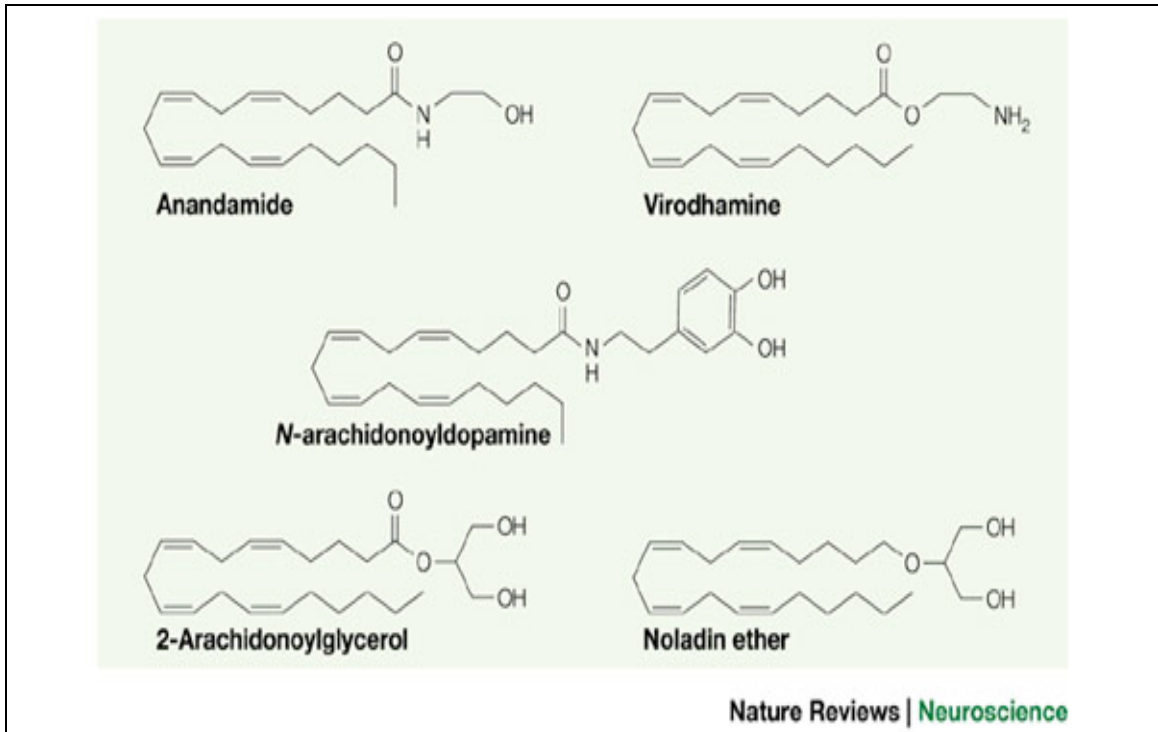


**Figure 6. Structures of endocannabinoids.** The two most important endocannabinoids are anandamide, also called N-arachidonyl ethanolamine (AEA), and 2-arachidonyl glycerol (2-AG). Figure taken from Piomelli, 2003.

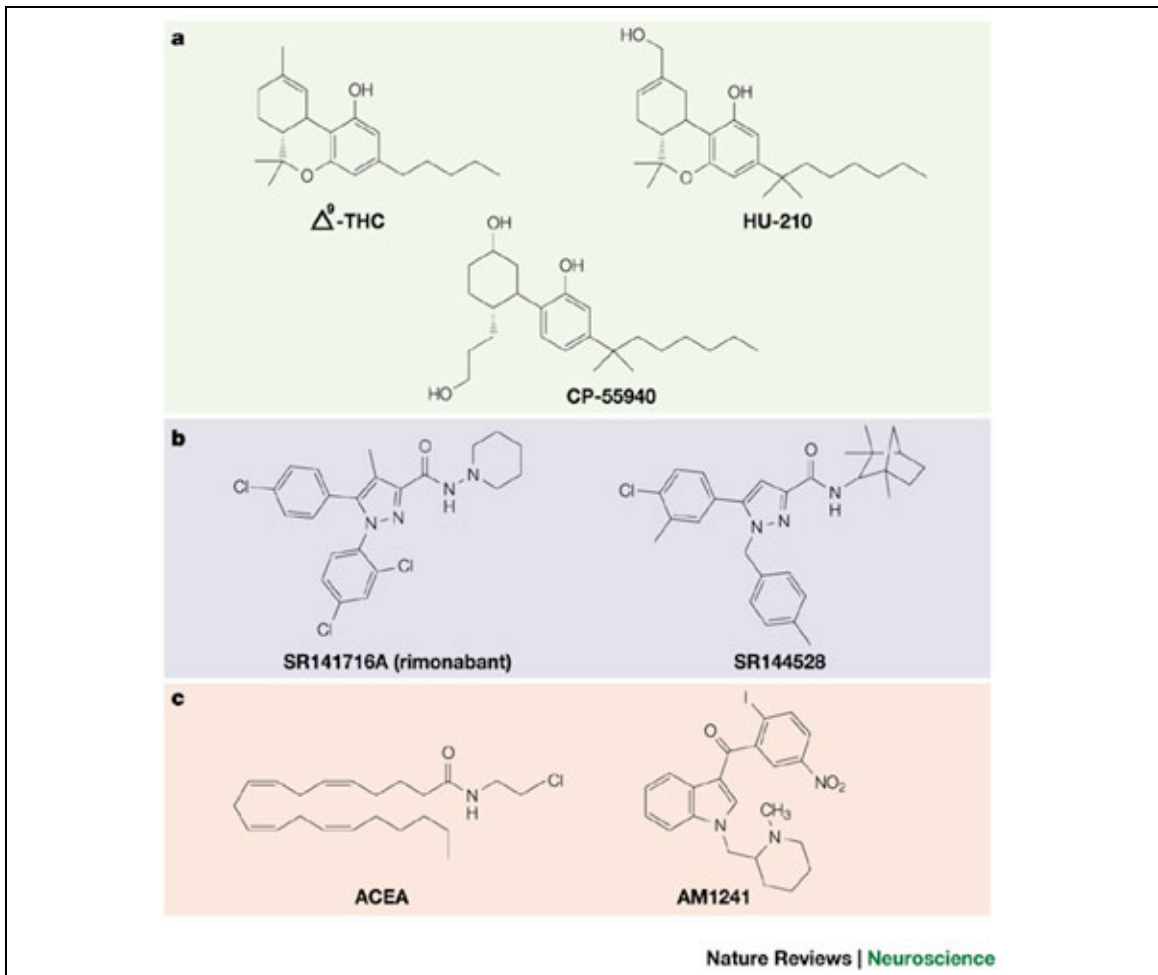


**Figure 7. Structures of exogenous cannabinoids.** A) Plant ( $\Delta^9$ -THC) and synthetic (HU-210 and CP-55940) nonselective cannabinoid agonists. B) Synthetic selective CB1 antagonist SR141716A (generic drug rimonabant) and synthetic selective CB2 antagonist SR144528. C) Synthetic selective CB1 agonist ACEA and synthetic selective CB2 agonist AM1241.  $\Delta^9$ -THC –  $\Delta^9$ -tetrahydrocannabinol; ACEA – arachidonyl-2'-chloroethylamide. Figure taken from Piomelli, 2003.

### **5.3 Rimonabant**

Rimonabant, a selective CB1 antagonist, was approved and marketed in Europe from 2006 to 2009 for indication of obesity [55]. The U.S. Food and Drug Administration (FDA) did not approve the drug because of adverse psychiatric effects including anxiety, depression, and suicidal ideation. Rimonabant was withdrawn from the European market in 2009 for the same reasons. Notwithstanding the psychiatric side effects, rimonabant was an effective drug. Rimonabant caused weight loss, decreased waist circumference, improved TAG and cholesterol levels, improved insulin sensitivity and glucose tolerance, and increased adiponectin levels [56].

### **5.4 Egr1**

Several groups have demonstrated Egr1 induction by CB1 agonists in non-adipose tissue. Boueboula et al. showed CB1 agonism by CP-55940 induced expression of Egr1 in human astrocytes [57]. Graham et al. showed CB1 agonism by HU210 induced Egr1 in an ERK-dependent manner in neuro2A neuronal cells [53]. Conversely, the same cells treated with CB1 antagonist SR141716A had decreased Egr1 expression. This finding raises the question of whether rimonabant's effects of improved insulin sensitivity and weight loss could be attributed, in part, to suppression of Egr1.

The mechanisms through which CB1 agonism and antagonism effect whole body metabolism are difficult to elucidate because CB1 is expressed both

centrally (in brain) and peripherally (in AT, liver, and muscle). Cota et al. demonstrated that age affects the extent to which central or peripheral CB1 controls metabolic state. They found that young CB1-null mice were lean secondary to reduced caloric intake, an effect mediated by the hypothalamus and other brain regions. Adult CB1-null mice were lean secondary to peripheral metabolic changes such as reduced lipogenesis in AT [58]. Trillou et al. found that compared to WT mice, CB1-null mice had 24 percent lower body weight and 60 percent lower adiposity on a normal diet at week 20 [59]. Furthermore, they found that high fat diet (HFD)-induced obesity does not occur in CB1-null mice. Again, these results are attributable to both central effects (decreased appetite and food intake in CB1-null mice) and peripheral effects (decreased adiposity). The extent to which CB1 induction of Egr1 contributes to these peripheral effects requires further investigation.

## **6. Thesis Objective**

Obesity and Type 2 Diabetes Mellitus are interlinked global health pandemics that demand exhaustive research. In the past two decades, the field has undergone a paradigm shift from framing diabetes as primarily a carbohydrate metabolism disorder to primarily a lipid metabolism disorder with secondary sugar consequences. The progression from mild insulin resistance to overt diabetes is now understood to involve dysregulation of plasma free fatty acid levels prior to glucose intolerance or hyperglycemia. This is the so-called

“lipotoxicity” model of insulin resistance. The Kandror Lab investigates the molecular mechanisms through which insulin suppresses lipolysis in adipose tissue, a fundamental signaling pathway that is defective in obesity and T2DM.

Recent work by the Kandror Lab has revealed mammalian target of rapamycin complex 1 (mTORC1) as a mediator of insulin’s antilipolytic effect in adipose tissue. Moreover, the lab has identified the transcription factor Egr1 as the mediator of mTORC1’s downregulation of adipose triglyceride lipase (ATGL), the rate-limiting lipolytic enzyme in adipose tissue. Several recent models illustrate how chronic hyperinsulinism in the pre-diabetic state leads to imbalance between PI3K-Akt and MAPK signal cascades in adipose tissue and results in adipose insulin resistance. These models are based on increased Egr1 expression in obesity.

Other groups have shown Egr1 to be a downstream effector of cannabinoid receptor 1 (CB1) in neurons. CB1 is also expressed in adipose tissue and is known to contribute to metabolic homeostasis. The endocannabinoid system is hyperactive in obesity and T2DM, and pharmacologic blockade of CB1 by the drug rimonabant was effective at weight loss, improving insulin sensitivity, and improving overall lipid metabolism. The specific goal of this project was to demonstrate for the first time that CB1 agonism induces Egr1 in adipocytes. Further investigation will be required to determine how CB1 agonism affects ATGL expression and lipolysis in adipose tissue.



## **MATERIALS AND METHODS**

### **3T3-L1 Adipocyte Differentiation**

Murine 3T3-L1 preadipocytes cultured in Dulbecco's modified Eagle's medium (DMEM) with 4.5 g/L glucose, L-glutamine, and sodium pyruvate (Cellgro 10-013-CV) supplemented with 10% donor bovine serum (Atlanta Biologicals S11350) and 1% penicillin-streptomycin-L-glutamine (Cellgro 30-009-CI). Cells incubated at 37°C and 10% CO<sub>2</sub>. Media replaced every 2-3 days.

At 2 days post-confluence (Day 0), media replaced with MDI induction media prepared as follows: DMEM with 4.5 g/L glucose, L-glutamine, and sodium pyruvate (Cellgro 10-013-CV) supplemented with 10% fetal bovine serum (Gibco 10437-028), 0.5 mM 3-isobutyl-1-methylxanthine (Sigma I-7018), 1 uM dexamethasone (Sigma D-4902), and 0.17 uM insulin (Sigma I-5500). At days 2, 4, and 6, media replaced with maintenance media (DMEM with 10% FBS). Cells incubated at 37°C and 10% CO<sub>2</sub>.

### **Human Adipocyte Differentiation**

Human adipocytes procured from subcutaneous adipose tissue were generously gifted by Mi-Jeong Lee, PhD, of the Fried Laboratory at Boston University School of Medicine. The adipocytes were received on Day 12 of differentiation in the following media: DMEM-F12 (Invitrogen 12500-062) with 17.5 mM glucose, 0.5 mM sodium pyruvate, and 2.5 mM L-glutamine,

supplemented with 100 units/ml penicillin-streptomycin, 25 mM sodium bicarbonate, 15 mM HEPES, 33 uM biotin, 17 uM pantothenic acid, 10 nM insulin, and 10 nM dexamethasone. Media was serum-free. Cells incubated at 37°C and 5% CO<sub>2</sub>.

### **Arachidonyl-2'-chloroethylamide (ACEA) Stimulation**

Murine 3T3-L1 adipocytes and human adipocytes were stimulated with 2 uM ACEA (Cayman 91054). ACEA, molecular weight 366 g/mol, was received as 5 mg dissolved in 500 ul methyl acetate. To 250 ul of the reagent, 250 ul dimethyl sulfoxide (American Bioanalytical AB0-3091) was added to create solution of 2.5 mg ACEA dissolved in 500 ul of 50% methyl acetate and 50% DMSO. To each of five 100 ul aliquots of this solution, 400 ul DMSO was added, to create solutions of 0.5 mg ACEA dissolved in 500 ul of 10% methyl acetate and 90% DMSO, for a final concentration of 2.73 mM ACEA. To stimulate adipocytes with 2 uM ACEA, 3.66 ul of 2.73 mM stock ACEA was added to cell culture dishes with 5 ml media. Murine 3T3-L1 adipocytes were serum-starved for 3 hours prior to ACEA stimulation. Human adipocytes were insulin- and dexamethasone-starved for 3 hours prior to ACEA stimulation.

### **Insulin Stimulation**

Murine 3T3-L1 adipocytes were stimulated with 100 nM insulin from bovine pancreas (Sigma I-5500), molecular weight 5733 g/mol. Insulin powder was dissolved in 0.02 M HCl to concentration 1 mg/ml, or 170 uM. To stimulate

adipocytes with 100 nM insulin, 3 ul of 170 uM stock insulin was added to cell culture dishes with 5 ml media. Cells were serum-starved for 3 hours prior to insulin stimulation.

### **Humulin Stimulation**

Human adipocytes were stimulated with 100 nM humulin (borrowed from Mi-Jeong Lee, PhD, of the Fried Laboratory at Boston University School of Medicine). Humulin was received as 60 uM stock solution. To stimulate adipocytes with 100 nM humulin, 8.3 ul of 60 uM stock humulin was added to cell culture dishes with 5 ml media. Cells were insulin- and dexamethasone-starved for 3 hours prior to humulin stimulation.

### **Western Blot Analysis of ATGL and Egr1 in Murine 3T3-L1 Adipocytes and Human Adipocytes**

Cells washed on culture dishes twice with 1X phosphate-buffered saline and placed on ice. Cells collected with cold lysis buffer (20 mM Tris-HCl at pH 7.4, 120 mM NaCl, 1% triton, 1 mM EGTA) supplemented with 1:100 protease inhibitor cocktail (Sigma P-8340) and 1:100 phosphatase inhibitor cocktail (Sigma P-0044). Cell lysates stored at -20°C. Cell lysate total protein concentration for Western blot analysis measured using a BCA assay kit (Thermo Scientific 23228 and 23224).

Proteins were prepared for SDS-polyacrylamide gel electrophoresis by mixing 15 ug total protein per well with additional lysis buffer to total volume of 20 ul per well. Each well sample received 5 ul 5X laemmli sample buffer (supplemented with 1:3  $\beta$ -mercaptoethanol), and all well samples were boiled at 95°C for 5 minutes prior to gel loading. ColorPlus prestained protein ladder (New England Biolabs P-7711S) was used as molecular weight marker.

Proteins were separated on 8% polyacrylamide gels prepared with 30% ProtoGel (National Diagnostics EC-890) and transferred to Immobilon-P Membranes (Millipore Corp. IPVH00010) in transfer buffer (25 mM Tris, 192 mM glycine) at 4°C. Following transfer, the membranes were washed three times in 1X PBS-Tween 20 (PBST) and blocked with 10% BSA in PBS with 0.5% Tween 20 for 1 hour. After three washes with PBST, blots were probed overnight with specific primary antibodies at 4°C. Primary antibodies: rabbit anti-ATGL (Cell Signal 2138), rabbit anti-Egr1 (Santa Cruz Biotechnology sc-110). After wash three times with PBST, blots incubated with horseradish peroxidase-conjugated secondary antibodies for 1 hour, and washed three times with PBST. Secondary antibodies: goat anti-rabbit IgG (Thermo Scientific 31460), goat anti-mouse IgG (Thermo Scientific 31430).

Protein bands were detected with the Western Lightning Plus-ECL Enhanced Chemiluminescence Substrate kit (PerkinElmer NEL104001EA) using the Bio-Rad Universal Hood II Gel Imager and corresponding software ImageLab Version 4.1.

## **RNA Extraction After Stimulation of Adipocytes**

RNA extracted from 3T3-L1 adipocytes and human adipocytes after stimulation by insulin, humulin, ACEA, or no stimulation. TRIzol reagent (Invitrogen 15596-026) added to plates to collect cell lysate, followed by addition of chloroform. After vigorous shaking and centrifugation at 12,000g for 15 min, top aqueous phase containing nucleic acid harvested and added to 2 volumes of isopropylalcohol. After vigorous shaking and centrifugation at 12,000g for 10 min, supernatant discarded and nucleic acid pellet washed with 75% ethanol, vortexed, centrifuged at 7,500g for 5 min, and air-dried 10 min. Pellet dissolved in 20 ul RNase-free water (distilled, autoclaved water with 0.1% diethylpyrocarbonate). RNA concentration measured using spectrophotometer.

RNA samples treated with DNase. To 10 ug RNA, final volume brought to 85 ul with DEPC-water. To each, 10 ul 10X DNase buffer (Invitrogen AM8170G) and 5 ul DNase I (Invitrogen AM2224) was added, and samples incubated at 37°C for 40 min. Following incubation, 200 ul DEPC-water and 300 ul phenol added, vortexed, and centrifuged. Upper aqueous layer containing RNA collected, 25 ul sodium acetate and 625 ul ethanol added, and samples stored overnight at -20°C. Samples centrifuged 15 min, supernatant removed, pellet washed with 75% ethanol, vortexed, centrifuged, supernatant removed, and air-dried 10 min. Finally, RNA pellet dissolved in 20 ul DEPC-water and stored at -70°C.

## **Reverse Transcription of RNA to cDNA**

Total RNA concentration measured using spectrophotometer. To 1 ug total RNA, DEPC-water added to volume of 10 ul, and 2 ul random decamers added. Samples heated to 80°C for 3 min on thermal cycler (MWG AG Biotech Primus 96 Plus). The remaining reverse transcription components added according to RETROScript kit (Ambion AM1710). Samples incubated on thermal cycler at 44°C for 1 hour, followed by 10 min incubation at 92°C to inactivate reverse transcriptase. Reaction tubes were 0.2 ml polypropylene PCR 8-tubes with clear caps (USA Scientific 1402-1900).

## **Analysis of mRNA Expression Using Quantitative Polymerase Chain**

### **Reaction**

Reaction components for qPCR mixed according to Brilliant II SYBR Green QPCR Master Mix (Agilent Technologies 410024). Briefly, 0.5 ul template cDNA added to 12.5 ul SYBR Green PCR Master Mix and 7 ul distilled water. Reaction tubes were Mx4000 8-tube strips and caps (Agilent Technologies 410022 and 410024). 5 ul primer mixture (3 ul forward and 3 ul reverse added to 94 ul distilled water) was added to each tube. Primers were as follows: mouse Egr1, forward 5'-CCACAACAACAGGGAGACCT-3' and reverse 5'-ACTGAGTGGCGAAGGCTTTA-3'; human Egr1, forward 5'-CCGCAGAGTCTTTTCCTGAC-3' and reverse 5'-TGGGTTGGTCATGCTCACTA-3' (Eurofins MWG Operon). All samples prepared

in triplicate. mRNA expression levels normalized to GAPDH mRNA in the murine 3T3-L1 adipocyte triplicate samples and to RPS18 mRNA in the human adipocyte triplicate samples. Primers for RPS18 mRNA (NM 022551.2) generously donated by Yasuo Ido, MD, PhD, of the Ruderman Laboratory at Boston University School of Medicine. Reactions were run at 95°C for 2 minutes followed by 30 cycles of 95°C for 2 minutes, 58°C for 30 seconds, and 72°C for 1 minute and finally ending with 1 cycle of 72°C for 5 minutes; reactions performed by Stratagene Mx4000 Multiplex Quantitative PCR System and corresponding software Mx4000 version 4.20.

### **qPCR Data Analysis and Statistics**

All qPCR tubes prepared in triplicate, and mRNA levels normalized to constitutively active genes glyceraldehyde 3-phosphate dehydrogenase (GAPDH) in murine cells or 40S ribosomal protein S18 (RPS18) in human cells. Expression of target mRNA (Egr1) set equal to 1.0 in non-stimulated (baseline) cells, and expression of target mRNA quantified as fold-increase above baseline in insulin-, humulin-, or ACEA-stimulated cells. Triplicate results averaged and bars represent standard deviation. Significance of difference in mRNA expression levels assessed using student's t-test.

## RESULTS

Because of recent discoveries by the Kandror Lab that mTORC1 induces Egr1 expression, and that Egr1 binds the ATGL promoter and decreases ATGL expression, we investigated the effect of CB1 stimulation on Egr1 and ATGL expression. To stimulate CB1, we used ACEA, a synthetic analogue of endocannabinoid AEA.

In murine 3T3-L1 adipocytes, stimulation with 2  $\mu$ M ACEA for 4 hours induced a 4.8-fold increase in Egr1 mRNA relative to control adipocytes receiving no ACEA (Figure 8), as determined by qPCR. All qPCR reactions were performed in triplicate, and mRNA levels were normalized to GAPDH mRNA. This mRNA expression change was statistically significant ( $p < 0.01$ ) as assessed by the student's t-test.

Total protein was also collected from 3T3-L1 adipocytes having undergone identical conditions, and levels of ATGL and Egr1 protein were assessed by Western blot. After 4 hours of CB1 stimulation with 2  $\mu$ M ACEA or no ACEA, there was no appreciable difference in ATGL or Egr1 protein levels (Figure 9). GAPDH protein was blotted as a loading control.

The experiment was repeated in cultured human adipocytes. A third condition was tested in these cells: 4 hour stimulation with 100 nM humulin. In these human adipocytes, 4 hour stimulation with 100 nM humulin increased Egr1 mRNA by a factor of 2.6 relative to control cells receiving no stimulation.



Moreover, 4 hour stimulation with 2  $\mu$ M ACEA increased Egr1 mRNA by a factor of 5.1 relative to control cells receiving no stimulation (Figure 10). Both of these mRNA expression changes were statistically significant ( $p < 0.05$ ) as assessed by the student's t-test. All qPCR reactions were performed in triplicate, and mRNA levels were normalized to RPS18 mRNA.

A separate trial was conducted where human adipocytes received either 4 hour or 16 hour CB1 stimulation with 2  $\mu$ M ACEA. Total protein was collected and levels of ATGL were assessed by Western blot. At both time points, ATGL protein was increased relative to cells receiving no ACEA (Figure 11). GAPDH protein was blotted as a loading control. We also blotted for Egr1 protein, but the gel produced an unreadable blot.

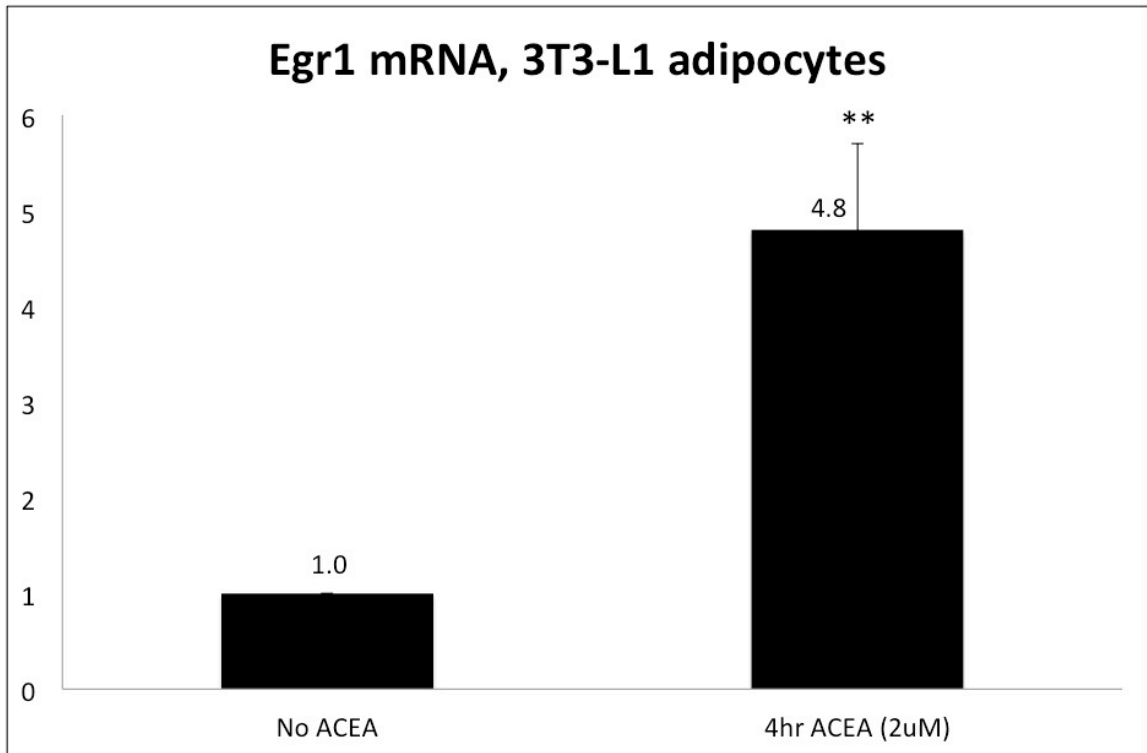


**Figure 8. ACEA induces Egr1 in murine 3T3-L1 adipocytes.** On day 6 of 3T3-L1 adipocyte differentiation, cells were serum-starved for 3 hours followed by stimulation with 2uM ACEA or no stimulation. After 4 hours, RNA was harvested and reverse transcribed to cDNA. qPCR samples were prepared in triplicate, and the bar represents standard deviation. mRNA levels were normalized to GAPDH mRNA levels. \*\* $p < 0.01$ . Egr1 – early growth responsive gene 1; ACEA – arachidonyl-2'-chloroethylamide; CB1 – cannabinoid receptor 1; GAPDH – glyceraldehyde 3-phosphate dehydrogenase.

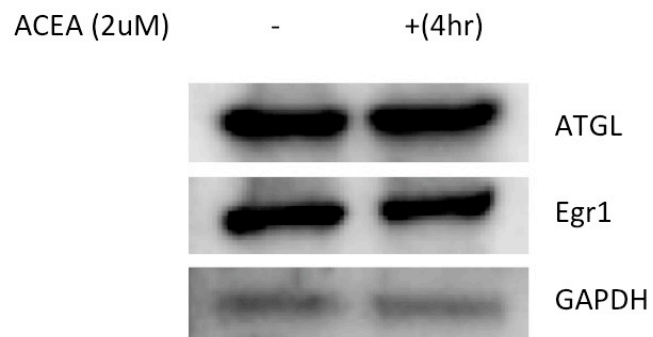


**Figure 9. ACEA does not affect Egr1 or ATGL protein.** On day 6 of 3T3-L1 adipocyte differentiation, cells were serum-starved for 3 hours followed by stimulation with 2uM ACEA or no stimulation. After 4 hours, cell lysate was harvested. GAPDH served as loading control. ATGL – adipose triglyceride lipase; Egr1 – early growth responsive gene 1; ACEA – arachidonyl-2'-chloroethylamide; CB1 – cannabinoid receptor 1; GAPDH – glyceraldehyde 3-phosphate dehydrogenase.

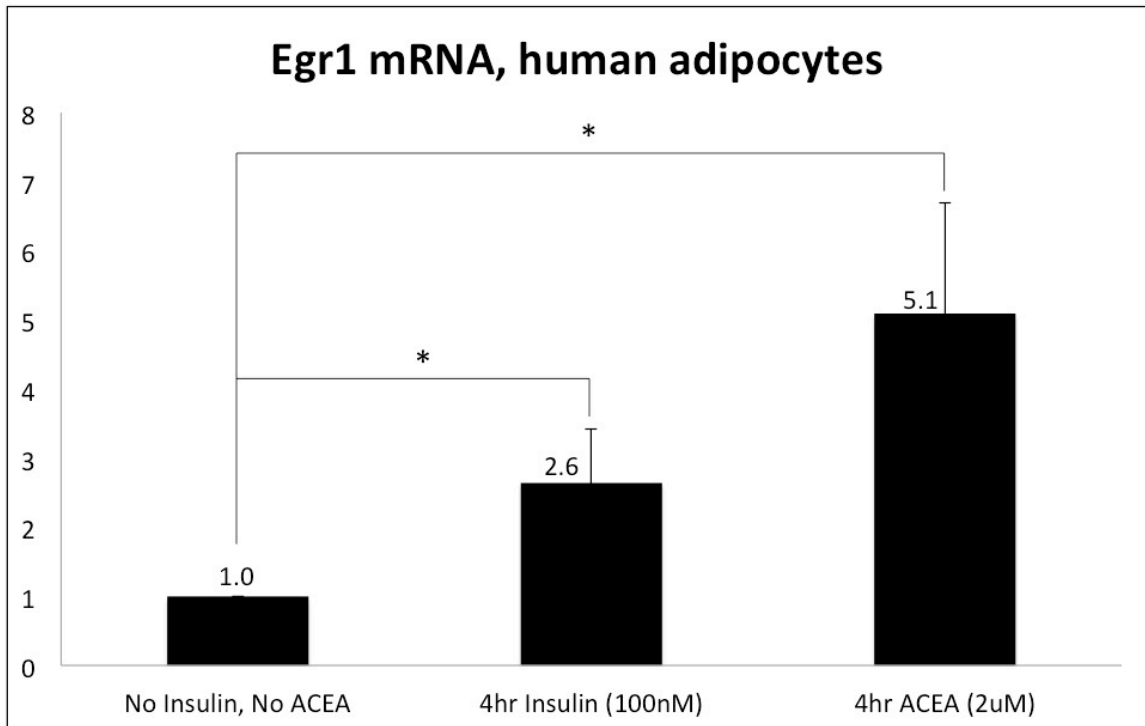


**Figure 10. Insulin and ACEA induce Egr1 in human adipocytes.** On day 13 of human adipocyte differentiation, cells were dexamethasone- and insulin-starved for 3 hours followed by stimulation with 100nM humulin or 2uM ACEA or no stimulation. After 4 hours, RNA was harvested and reverse transcribed to cDNA. qPCR samples were prepared in triplicate, and the bars represent standard deviation. mRNA levels were normalized to RPS18 mRNA levels. \* $p < 0.05$ . Egr1 – early growth responsive gene 1; ACEA – arachidonyl-2'-chloroethylamide; CB1 – cannabinoid receptor 1; RPS18 – 40S ribosomal protein S18.

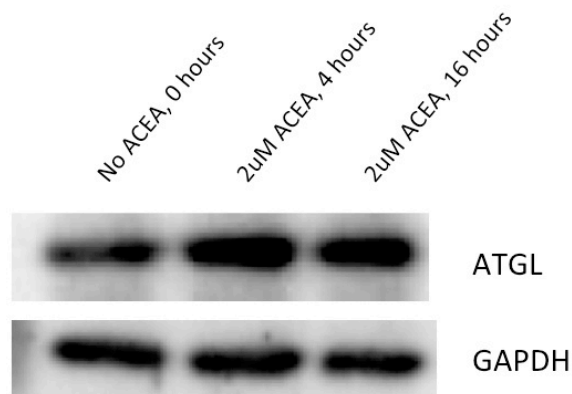


**Figure 11. ACEA increases ATGL protein in human adipocytes.** On day 13 of human adipocyte differentiation, cells were dexamethasone- and insulin-starved for 3 hours followed by stimulation with 2uM ACEA or no stimulation. After 0, 4, and 16 hours, cell lysate was harvested. GAPDH served as loading control. ATGL – adipose triglyceride lipase; ACEA – arachidonyl-2'-chloroethylamide; CB1 – cannabinoid receptor 1; GAPDH – glyceraldehyde 3-phosphate dehydrogenase.

## DISCUSSION

Several recent discoveries led us to test the effect of CB1 stimulation on Egr1 and ATGL expression in adipocytes. ATGL, the rate-limiting lipolytic enzyme in adipose tissue, is downregulated in the insulin-stimulated state, and this antilipolytic signal is defective in obesity and T2DM and may contribute to lipotoxicity [24]. The antilipolytic effect of insulin on AT is mediated by mTORC1 [36]. Recently, the Kandror Lab identified the transcription factor Egr1 as the

mediator between activated mTORC1 and decreased ATGL transcription (unpublished data). Activated mTORC1 increases the expression of Egr1 mRNA and protein, and Egr1 binds the ATGL promoter and decreases transcription of ATGL. This is an evolutionarily conserved interaction and is documented in yeast, fruit fly, and mice (unpublished data).

Egr1 has recently been implicated in several new models of the pathogenesis of adipose tissue insulin resistance in the pre-diabetic hyperinsulinemic state [37] [49]. These authors assert that chronic hyperinsulinism causes an imbalance between PI3K/Akt signaling and MAPK signaling. Specifically, high levels of Egr1 in obesity and diabetes increase MAPK signaling via increased Ras prenylation, an effect of Egr1 transactivation of the GGPS gene. Concurrently, Egr1 transactivates the PTEN gene, an inhibitor of PI3K/Akt signaling. Overactive ERK (MAPK) phosphorylates and inactivates IRS1, which also diminishes PI3K/Akt signaling. Diminished PI3K/Akt signaling decreases insulin-stimulated GLUT4 translocation to the cell surface and decreases plasma glucose clearance in the fed state.

The endocannabinoid system (ECS) is known to be overactive in obesity and diabetes [52], and CB1 antagonism by the drug rimonabant was effective at decreasing weight and improving insulin resistance in overweight and obese patients [56]. It is conceivable that overactive ECS in obesity could contribute to the development of insulin resistance, and we sought to determine the effects of CB1 stimulation on Egr1 expression. Previous research demonstrated induction

of Egr1 by CB1 stimulation in neurons [57] [53], however the induction of Egr1 by CB1 stimulation has not been demonstrated in adipocytes.

By using quantitative PCR, we were able to assess the change in Egr1 mRNA levels in CB1-stimulated murine 3T3-L1 adipocytes and human adipocytes relative to non-stimulated control adipocytes. In both cell types, stimulation with 2  $\mu$ M ACEA (a synthetic analogue of endocannabinoid AEA and a specific CB1 agonist) significantly induced Egr1 mRNA after 4 hours (Figures 8 and 10). Stimulation of human adipocytes with 100 nM humulin also significantly induced Egr1 mRNA, although to a lesser extent than did ACEA.

Western blot analysis showed no change in Egr1 or ATGL protein levels after 4 hours of ACEA stimulation in murine 3T3-L1 adipocytes (Figure 9). This result corresponds to previous data from the Kandror Lab showing no increase in Egr1 protein until 8 hours of insulin stimulation, and no decrease in ATGL protein until 16 hours of insulin stimulation. Figure 9 is in agreement with the finding that Egr1 mRNA increase precedes Egr1 protein increase by hours, and Egr1 protein increase precedes ATGL mRNA and protein decrease by hours (unpublished Kandror data).

The one surprising result was the increase of ATGL protein in 4-hour and 16-hour ACEA stimulated human adipocytes (Figure 11). This result runs counter to the previous finding that increasing Egr1 mRNA leads to decreased ATGL expression. A closer examination of the components of the human adipocyte media (which was kindly donated by Mi-Jeong Lee, PhD, of the Fried Laboratory

and was much more complex than our typical murine 3T3-L1 media) is necessary to assess for confounding factors. Unfortunately, the Egr1 blot was unreadable due to gel abnormalities. The experiment requires repeating.

A necessary future experiment would be a time course similar to the one described in the unpublished Kandror data. Egr1 and ATGL mRNA and protein should be measured at 4-, 8-, and 16-hour ACEA stimulation. It is logical that the results of that future experiment would mirror the results of the insulin time course described in the Introduction section. A second future experiment worth performing is a similar time course experiment and measurement of Egr1 and ATGL mRNA and protein, except using CB1 antagonist SR141716A (rimonabant). Logically, the result should be reversed: Egr1 expression should decrease, followed by an ATGL increase.

Future investigation is also necessary to dissect the pathways through which CB1 stimulation induces Egr1. CB1 activates the MAPK pathway [54], but is ERK the dominant stimulator of Egr1 expression, or is mTORC1 the major mediator? (ERK induces Egr1 directly and also activates mTORC1, and mTORC1 induces Egr1 independently of ERK.) Furthermore, elucidation of CB1 signal transduction in adipocytes is crucial for the future development of peripheral-specific drugs that bind CB1. The major downfall of the otherwise highly effective rimonabant was the adverse psychiatric effects, which would be attenuated by cannabinoid drugs designed for brain exclusion.



Finally, the sequence of events in obesity and T2DM disease progression remains somewhat perplexing. Some of the research findings are counter-intuitive and portend even greater complexity than is currently understood. For example, insulin resistant adipose tissue has defective antilipolytic signal, yet ATGL expression is decreased in obese and diabetic patients and ob/ob and db/db mice [22]. Decreased ATGL expression in these disease states would be expected to decrease plasma FFA and lipotoxicity, but the opposite is true. These and other seemingly contradictory findings will continue to fuel research in the “diabesity” epidemic for quite awhile.

## REFERENCES

- [1] Editorial, "The Diabetes Pandemic," *The Lancet*, vol. 378, no. 9786, p. 99, Jul. 2011.
- [2] M. Best, "The Growing Challenge of 'Diabesity'," *NIH Medline Plus*, vol. 3, no. 1, p. 12, Winter-2008.
- [3] Centers for Disease Control and Prevention, "National Diabetes Fact Sheet: National estimates and general information on diabetes and prediabetes in the United States, 2011," U.S. Department of Health and Human Services, Centers for Disease Control and Prevention, Atlanta, GA, 2011.
- [4] Centers for Disease Control and Prevention, "Long-Term Trends in Diagnosed Diabetes," CDC Division of Diabetes Translation, 01-Oct-2011.
- [5] D. L. Hoyert and J. Xu, "Deaths: Preliminary Data for 2011," U.S. Department of Health and Human Services, Centers for Disease Control and Prevention, Atlanta, GA, Vol. 61 No. 6, Oct. 2012.
- [6] J. D. McGarry, "What if Minkowski had been ageusic? An alternative angle on diabetes," *Science*, vol. 258, no. 5083, pp. 766–770, Oct. 1992.
- [7] D. B. Savage, K. F. Petersen, and G. I. Shulman, "Disordered Lipid Metabolism and the Pathogenesis of Insulin Resistance," *Physiological Reviews*, vol. 87, no. 2, pp. 507–520, Apr. 2007.
- [8] Y. Lee, H. Hirose, M. Ohneda, J. H. Johnson, J. D. McGarry, and R. H. Unger, "Beta-cell lipotoxicity in the pathogenesis of non-insulin-dependent diabetes mellitus of obese rats: impairment in adipocyte-beta-cell relationships," *Proceedings of the National Academy of Sciences*, vol. 91, no. 23, pp. 10878–10882, 1994.
- [9] R. H. Unger, "Lipotoxicity in the pathogenesis of obesity-dependent NIDDM. Genetic and clinical implications.," *Diabetes*, vol. 44, no. 8, pp. 863–70, Aug. 1995.
- [10] A. Dresner, D. Laurent, M. Marcucci, M. E. Griffin, S. Dufour, G. W. Cline, L. A. Slezak, D. K. Andersen, R. S. Hundal, and D. L. Rothman, "Effects of free fatty acids on glucose transport and IRS-1-associated phosphatidylinositol 3-kinase activity," *Journal of Clinical Investigation*, vol. 103, pp. 253–260, 1999.
- [11] R. H. Unger, G. O. Clark, P. E. Scherer, and L. Orci, "Lipid homeostasis, lipotoxicity and the metabolic syndrome," *Biochimica et Biophysica Acta*

- (*BBA*) - *Molecular and Cell Biology of Lipids*, vol. 1801, no. 3, pp. 209–214, Mar. 2010.
- [12] S. Kashyap, R. Belfort, A. Gastaldelli, T. Pratipanawatr, R. Berria, W. Pratipanawatr, M. Bajaj, L. Mandarino, R. DeFronzo, and K. Cusi, “A sustained increase in plasma free fatty acids impairs insulin secretion in nondiabetic subjects genetically predisposed to develop type 2 diabetes,” *Diabetes*, vol. 52, no. 10, pp. 2461–2474, 2003.
- [13] G. Boden and G. I. Shulman, “Free fatty acids in obesity and type 2 diabetes: defining their role in the development of insulin resistance and  $\beta$ -cell dysfunction,” *European Journal of Clinical Investigation*, vol. 32, no. s3, pp. 14–23, 2002.
- [14] H. Bays, L. Mandarino, and R. A. DeFronzo, “Role of the Adipocyte, Free Fatty Acids, and Ectopic Fat in Pathogenesis of Type 2 Diabetes Mellitus: Peroxisomal Proliferator-Activated Receptor Agonists Provide a Rational Therapeutic Approach,” *Journal of Clinical Endocrinology & Metabolism*, vol. 89, no. 2, pp. 463–478, Feb. 2004.
- [15] M.-A. Cornier, D. Dabelea, T. L. Hernandez, R. C. Lindstrom, A. J. Steig, N. R. Stob, R. E. Van Pelt, H. Wang, and R. H. Eckel, “The Metabolic Syndrome,” *Endocrine Reviews*, vol. 29, no. 7, pp. 777–822, Aug. 2008.
- [16] R. A. DeFronzo, “Insulin resistance, lipotoxicity, type 2 diabetes and atherosclerosis: the missing links. The Claude Bernard Lecture 2009,” *Diabetologia*, vol. 53, no. 7, pp. 1270–1287, Apr. 2010.
- [17] C. Londos, D. L. Brasaemle, C. J. Schultz, J. P. Segrest, and A. R. Kimmel, “Perilipins, ADRP, and other proteins that associate with intracellular neutral lipid droplets in animal cells,” *Seminars in Cell & Developmental Biology*, vol. 10, no. 1, pp. 51–58, Feb. 1999.
- [18] M. Vaughan, J. E. Berger, and D. Steinberg, “Hormone-sensitive lipase and monoglyceride lipase activities in adipose tissue,” *Journal of Biological Chemistry*, vol. 239, no. 2, pp. 401–409, 1964.
- [19] G. Haemmerle, R. Zimmermann, M. Hayn, C. Theussl, G. Waeg, E. Wagner, W. Sattler, T. M. Magin, E. F. Wagner, and R. Zechner, “Hormone-sensitive Lipase Deficiency in Mice Causes Diglyceride Accumulation in Adipose Tissue, Muscle, and Testis,” *Journal of Biological Chemistry*, vol. 277, no. 7, pp. 4806–4815, Nov. 2001.
- [20] C. M. Jenkins, D. J. Mancuso, W. Yan, H. F. Sims, B. Gibson, and R. W. Gross, “Identification, Cloning, Expression, and Purification of Three Novel

- Human Calcium-independent Phospholipase A2 Family Members Possessing Triacylglycerol Lipase and Acylglycerol Transacylase Activities," *Journal of Biological Chemistry*, vol. 279, no. 47, pp. 48968–48975, Aug. 2004.
- [21] R. Zimmermann, J. G. Strauss, G. Haemmerle, G. Schoiswohl, R. Birner-Gruenberger, M. Riederer, A. Lass, G. Neuberger, F. Eisenhaber, A. Hermetter, and R. Zechner, "Fat Mobilization in Adipose Tissue Is Promoted by Adipose Triglyceride Lipase," *Science*, vol. 306, no. 5700, pp. 1383–1386, Nov. 2004.
- [22] J. A. Villena, S. Roy, E. Sarkadi-Nagy, K. H. Kim, and H. S. Sul, "Desnutrin, an Adipocyte Gene Encoding a Novel Patatin Domain-containing Protein, Is Induced by Fasting and Glucocorticoids: Ectopic Expression of Desnutrin Increases Triglyceride Hydrolysis," *Journal of Biological Chemistry*, vol. 279, no. 45, pp. 47066–47075, Aug. 2004.
- [23] M. Schweiger, R. Schreiber, G. Haemmerle, A. Lass, C. Fledelius, P. Jacobsen, H. Tornqvist, R. Zechner, and R. Zimmermann, "Adipose Triglyceride Lipase and Hormone-sensitive Lipase Are the Major Enzymes in Adipose Tissue Triacylglycerol Catabolism," *Journal of Biological Chemistry*, vol. 281, no. 52, pp. 40236–40241, Nov. 2006.
- [24] P. Chakrabarti and K. V. Kandror, "Adipose Triglyceride Lipase: A New Target in the Regulation of Lipolysis by Insulin," *Current Diabetes Reviews*, vol. 7, no. 4, pp. 270–7, Jul. 2011.
- [25] G. Haemmerle, A. Lass, R. Zimmermann, G. Gorkiewicz, C. Meyer, J. Rozman, G. Heidmaier, R. Maier, C. Theussl, S. Eder, D. Kratky, E. F. Wagner, M. Klingenspor, G. Hoefler, and R. Zechner, "Defective Lipolysis and Altered Energy Metabolism in Mice Lacking Adipose Triglyceride Lipase," *Science*, vol. 312, no. 5774, pp. 734–737, May 2006.
- [26] A. J. Hoy, C. R. Bruce, S. M. Turpin, A. J. Morris, M. A. Febbraio, and M. J. Watt, "Adipose Triglyceride Lipase-Null Mice Are Resistant to High-Fat Diet-Induced Insulin Resistance Despite Reduced Energy Expenditure and Ectopic Lipid Accumulation," *Endocrinology*, vol. 152, no. 1, pp. 48–58, Nov. 2010.
- [27] M. Ahmadian, R. E. Duncan, K. A. Varady, D. Frasson, M. K. Hellerstein, A. L. Birkenfeld, V. T. Samuel, G. I. Shulman, Y. Wang, C. Kang, and H. S. Sul, "Adipose Overexpression of Desnutrin Promotes Fatty Acid Use and Attenuates Diet-Induced Obesity," *Diabetes*, vol. 58, no. 4, pp. 855–866, Jan. 2009.

- [28] R. Zechner, R. Zimmermann, T. O. Eichmann, S. D. Kohlwein, G. Haemmerle, A. Lass, and F. Madeo, "FAT SIGNALS - Lipases and Lipolysis in Lipid Metabolism and Signaling," *Cell Metabolism*, vol. 15, no. 3, pp. 279–291, Mar. 2012.
- [29] A. Lass, R. Zimmermann, G. Haemmerle, M. Riederer, G. Schoiswohl, M. Schweiger, P. Kienesberger, J. G. Strauss, G. Gorkiewicz, and R. Zechner, "Adipose triglyceride lipase-mediated lipolysis of cellular fat stores is activated by CGI-58 and defective in Chanarin-Dorfman Syndrome," *Cell Metabolism*, vol. 3, no. 5, pp. 309–319, May 2006.
- [30] X. Yang, X. Zhang, B. L. Heckmann, X. Lu, and J. Liu, "Relative Contribution of Adipose Triglyceride Lipase and Hormone-sensitive Lipase to Tumor Necrosis Factor- (TNF- )-induced Lipolysis in Adipocytes," *Journal of Biological Chemistry*, vol. 286, no. 47, pp. 40477–40485, Oct. 2011.
- [31] J. E. Campbell, A. J. Peckett, A. M. D'souza, T. J. Hawke, and M. C. Riddell, "Adipogenic and lipolytic effects of chronic glucocorticoid exposure," *AJP: Cell Physiology*, vol. 300, no. 1, pp. C198–C209, Oct. 2010.
- [32] P. Chakrabarti, T. English, S. Karki, L. Qiang, R. Tao, J. Kim, Z. Luo, S. R. Farmer, and K. V. Kandror, "SIRT1 controls lipolysis in adipocytes via FOXO1-mediated expression of ATGL," *The Journal of Lipid Research*, vol. 52, no. 9, pp. 1693–1701, Jul. 2011.
- [33] B. D. Manning and L. C. Cantley, "AKT/PKB Signaling: Navigating Downstream," *Cell*, vol. 129, no. 7, pp. 1261–1274, Jun. 2007.
- [34] T. Kitamura, Y. Kitamura, S. Kuroda, Y. Hino, M. Ando, K. Kotani, H. Konishi, H. Matsuzaki, U. Kikkawa, and W. Ogawa, "Insulin-induced phosphorylation and activation of cyclic nucleotide phosphodiesterase 3B by the serine-threonine kinase Akt," *Molecular and cellular biology*, vol. 19, no. 9, pp. 6286–6296, 1999.
- [35] P. Chakrabarti and K. V. Kandror, "FoxO1 Controls Insulin-dependent Adipose Triglyceride Lipase (ATGL) Expression and Lipolysis in Adipocytes," *Journal of Biological Chemistry*, vol. 284, no. 20, pp. 13296–13300, Mar. 2009.
- [36] P. Chakrabarti, T. English, J. Shi, C. M. Smas, and K. V. Kandror, "Mammalian Target of Rapamycin Complex 1 Suppresses Lipolysis, Stimulates Lipogenesis, and Promotes Fat Storage," *Diabetes*, vol. 59, no. 4, pp. 775–781, Jan. 2010.

- [37] N. Shen, X. Yu, F.-Y. Pan, X. Gao, B. Xue, and C.-J. Li, "An Early Response Transcription Factor, Egr-1, Enhances Insulin Resistance in Type 2 Diabetes with Chronic Hyperinsulinism," *Journal of Biological Chemistry*, vol. 286, no. 16, pp. 14508–14515, Feb. 2011.
- [38] L. Qiao, B. Kinney, J. Schaack, and J. Shao, "Adiponectin Inhibits Lipolysis in Mouse Adipocytes," *Diabetes*, vol. 60, no. 5, pp. 1519–1527, Mar. 2011.
- [39] S. Karki, P. Chakrabarti, G. Huang, H. Wang, S. R. Farmer, and K. V. Kandror, "The Multi-Level Action of Fatty Acids on Adiponectin Production by Fat Cells," *PLoS ONE*, vol. 6, no. 11, p. e28146, Nov. 2011.
- [40] T. Geetha, C. Zheng, N. Vishwaprakash, T. L. Broderick, and J. R. Babu, "Sequestosome 1/p62, a Scaffolding Protein, Is a Newly Identified Partner of IRS-1 Protein," *Journal of Biological Chemistry*, vol. 287, no. 35, pp. 29672–29678, Jul. 2012.
- [41] K. G. Foster and D. C. Fingar, "Mammalian Target of Rapamycin (mTOR): Conducting the Cellular Signaling Symphony," *Journal of Biological Chemistry*, vol. 285, no. 19, pp. 14071–14077, Mar. 2010.
- [42] P. T. Bhaskar and N. Hay, "The Two TORCs and Akt," *Developmental Cell*, vol. 12, no. 4, pp. 487–502, Apr. 2007.
- [43] M. Schweiger, M. Paar, C. Eder, J. Brandis, E. Moser, G. Gorkiewicz, S. Grond, F. P. W. Radner, I. Cerik, I. Cornaciu, M. Oberer, S. Kersten, R. Zechner, R. Zimmermann, and A. Lass, "G0/G1 switch gene-2 regulates human adipocyte lipolysis by affecting activity and localization of adipose triglyceride lipase," *The Journal of Lipid Research*, vol. 53, no. 11, pp. 2307–2317, Aug. 2012.
- [44] J. Eguchi, X. Wang, S. Yu, E. E. Kershaw, P. C. Chiu, J. Dushay, J. L. Estall, U. Klein, E. Maratos-Flier, and E. D. Rosen, "Transcriptional Control of Adipose Lipid Handling by IRF4," *Cell Metabolism*, vol. 13, no. 3, pp. 249–259, Mar. 2011.
- [45] J. Y. Kim, K. Tillison, J. H. Lee, D. A. Rearick, and C. M. Smas, "The adipose tissue triglyceride lipase ATGL/PNPLA2 is downregulated by insulin and TNF- $\alpha$  in 3T3-L1 adipocytes and is a target for transactivation by PPAR," *AJP: Endocrinology and Metabolism*, vol. 291, no. 1, pp. E115–E127, Feb. 2006.
- [46] E. E. Kershaw, M. Schupp, H.-P. Guan, N. P. Gardner, M. A. Lazar, and J. S. Flier, "PPAR $\alpha$  regulates adipose triglyceride lipase in adipocytes in vitro

- and in vivo," *AJP: Endocrinology and Metabolism*, vol. 293, no. 6, pp. E1736–E1745, Oct. 2007.
- [47] J. Huang and B. D. Manning, "The TSC1–TSC2 complex: a molecular switchboard controlling cell growth," *Biochemical Journal*, vol. 412, no. 2, p. 179, Jun. 2008.
- [48] M. Ahmadian, Y. Wang, and H. S. Sul, "Lipolysis in adipocytes," *The International Journal of Biochemistry & Cell Biology*, vol. 42, no. 5, pp. 555–559, May 2010.
- [49] X. Yu, N. Shen, M.-L. Zhang, F.-Y. Pan, C. Wang, W.-P. Jia, C. Liu, Q. Gao, X. Gao, and B. Xue, "Egr-1 decreases adipocyte insulin sensitivity by tilting PI3K/Akt and MAPK signal balance in mice," *The EMBO Journal*, vol. 30, no. 18, pp. 3754–3765, 2011.
- [50] P. Sartipy and D. J. Loskutoff, "Expression Profiling Identifies Genes That Continue to Respond to Insulin in Adipocytes Made Insulin-resistant by Treatment with Tumor Necrosis Factor- $\alpha$ ," *Journal of Biological Chemistry*, vol. 278, no. 52, pp. 52298–52306, Oct. 2003.
- [51] D. H. Nam, M. H. Lee, J. E. Kim, H. K. Song, Y. S. Kang, J. E. Lee, H. W. Kim, J. J. Cha, Y. Y. Hyun, S. H. Kim, S. Y. Han, K. H. Han, J. Y. Han, and D. R. Cha, "Blockade of Cannabinoid Receptor 1 Improves Insulin Resistance, Lipid Metabolism, and Diabetic Nephropathy in db/db Mice," *Endocrinology*, vol. 153, no. 3, pp. 1387–1396, Jan. 2012.
- [52] U. Pagotto, G. Marsicano, D. Cota, B. Lutz, and R. Pasquali, "The Emerging Role of the Endocannabinoid System in Endocrine Regulation and Energy Balance," *Endocrine Reviews*, vol. 27, no. 1, pp. 73–100, Sep. 2005.
- [53] E. S. Graham, N. Ball, E. L. Scotter, P. Narayan, M. Dragunow, and M. Glass, "Induction of Krox-24 by Endogenous Cannabinoid Type 1 Receptors in Neuro2A Cells Is Mediated by the MEK-ERK MAPK Pathway and Is Suppressed by the Phosphatidylinositol 3-Kinase Pathway," *Journal of Biological Chemistry*, vol. 281, no. 39, pp. 29085–29095, Aug. 2006.
- [54] D. Piomelli, "The molecular logic of endocannabinoid signalling," *Nature Reviews Neuroscience*, vol. 4, no. 11, pp. 873–884, Nov. 2003.
- [55] J. G. Kang and C.-Y. Park, "Anti-Obesity Drugs: A Review about Their Effects and Safety," *Diabetes & Metabolism Journal*, vol. 36, no. 1, p. 13, 2012.

- [56] J.-P. Després, A. Golay, and L. Sjöström, “Effects of rimonabant on metabolic risk factors in overweight patients with dyslipidemia,” *New England Journal of Medicine*, vol. 353, no. 20, pp. 2121–2134, 2005.
- [57] M. Bouaboula, B. Bourrie, M. Rinaldi-Carmona, D. Shire, G. Le Fur, and P. Casellas, “Stimulation of cannabinoid receptor CB1 induces krox-24 expression in human astrocytoma cells,” *Journal of Biological Chemistry*, vol. 270, no. 23, pp. 13973–80, Jun. 1995.
- [58] D. Cota, G. Marsicano, M. Tschöp, Y. Grübler, C. Flachskamm, M. Schubert, D. Auer, A. Yassouridis, C. Thöne-Reineke, S. Ortmann, F. Tomassoni, C. Cervino, E. Nisoli, A. C. E. Linthorst, R. Pasquali, B. Lutz, G. K. Stalla, and U. Pagotto, “The endogenous cannabinoid system affects energy balance via central orexigenic drive and peripheral lipogenesis,” *Journal of Clinical Investigation*, vol. 112, no. 3, pp. 423–431, Aug. 2003.
- [59] C. Ravinet Trillou, C. Delgorge, C. Menet, M. Arnone, and P. Soubrié, “CB1 cannabinoid receptor knockout in mice leads to leanness, resistance to diet-induced obesity and enhanced leptin sensitivity,” *International Journal of Obesity*, vol. 28, no. 4, pp. 640–648, Feb. 2004.



VITA

[REDACTED]

[REDACTED]

[REDACTED]

[REDACTED]

[REDACTED]

[REDACTED]

[REDACTED]

[REDACTED]

[REDACTED]

[REDACTED]

[REDACTED]

[REDACTED]

[REDACTED]

[REDACTED]

[REDACTED]

[REDACTED]